SLAC-PUB-7745
UMN-D-98-1
SMUHEP/98-01

Pauli–Villars as a Nonperturbative Ultraviolet Regulator in Discretized Light-Cone Quantization

Stanley J. Brodsky*
Stanford Linear Accelerator Center, Stanford University, Stanford, California 94309

John R. Hiller
Department of Physics, University of Minnesota, Duluth, Minnesota 55812

Gary McCartor†
Department of Physics, Southern Methodist University, Dallas, Texas 75275
(February 16, 1998)

Abstract

We propose a solution to the problem of renormalizing light-cone Hamiltonian theories while maintaining Lorentz invariance and other symmetries. The method uses generalized Pauli–Villars regulators to render the theory finite. We discuss the method in the context of Yukawa theory at one loop and for a soluble model in $3+1$ dimensions. The model is studied nonperturbatively. Numerical results obtained with use of discretized light-cone quantization, special integration weighting factors, and the complex symmetric Lanczos diagonalization algorithm compare well with the analytic answers.

12.38.Lg,11.15.Tk,11.10.Gh,02.60.Nm

(Submitted to Physical Review D.)

*Work supported in part by the Department of Energy, contract DE-AC03-76SF00515.

†Work supported in part by the Department of Energy, contract DE-FG03-95ER40908.

I. INTRODUCTION

DLCQ (Discretized Light-Cone Quantization) [1–3] is a suggested computational procedure in which one specifies quantization conditions on the characteristic surface $x^+ \equiv (x^0 + x^1) = 0$, introduces periodicity conditions to induce a discrete basis, truncates the basis set by some procedure to produce a finite matrix, then takes the spectrum and eigenvectors of that matrix as an approximation to the physical spectrum and wave functions. The difficulty is that, as always in quantum field theory, removing an infinite set of high (bare) energy states induces a renormalization of the operators. A completely consistent procedure for performing the truncation and renormalization has not yet been demonstrated, but the problem has received considerable study. Some calculations have been published [4] which simply use the periodicity conditions combined with a momentum cutoff. While the numerical results are accurate for superrenormalizable theories such as $1+1$-dimensional gauge theories, it is clear that such a procedure is problematical for renormalizable theories in $3+1$ dimensions. A systematic renormalization procedure has been proposed by Wilson, Perry and co-workers [5]. These authors use a cutoff chosen for computational convenience and then try to find the mixing of the operators under renormalization using ideas of the Wilson renormalization group. Since the procedure makes no attempt to preserve the symmetries of the theory, one expects a great deal of mixing and many counterterms; some skill in guessing the counterterms seems to be required.

In this paper we will suggest a procedure which lies somewhat closer to traditional ideas in field theory than the Wilson plan in that we will make an attempt to preserve more of the symmetries of the theory; but the objective is the same. The idea is to add enough Pauli–Villars fields [6] to the theory to regulate perturbation theory. Having done that we hope that, since the theory is basically finite, the periodicity conditions and momentum cutoff will be sufficiently benign to allow a consistent renormalization to be performed. In the Wilson language, we hope that the heavy fields will add the necessary counterterms automatically with no particular cleverness from us.

In the next section we consider the one-loop fermion self mass in Yukawa theory [7]. This problem has been considered previously in the literature [8], but we shall discuss the analysis in the context of using the Pauli–Villars program to preserve the discrete chiral symmetry of the theory. The computation requires three Pauli–Villars fields for proper regularization, including the elimination of all terms — including spurious finite terms — not proportional to the bare fermion mass squared.

We then present and solve a model field theory very similar to the scalar field model studied in the 1950's by Greenberg and Schweber [9]. This model, which requires renormalization, allows us to illustrate the procedure and to examine some important numerical issues, at least within the context of the model. These issues include the number of states which must be devoted to the heavy fields and the related question of how heavy their masses must be. Section IV discusses the numerical solution of this same model and compares these results with the analytic solution.

A final section contains our general conclusions. This is followed by two appendices that provide details of our light-cone conventions and of improved methods for accurate DLCQ calculations.

II. REGULARIZATION OF THE FERMION SELF-ENERGY IN LIGHT-CONE QUANTIZATION

A. Analysis

We consider Yukawa theory defined by the action

$$S = \int d^4x \left[\frac{1}{2}(\partial_\mu \phi)^2 - \frac{1}{2}\mu^2\phi^2 + \frac{i}{2}\big(\overline{\psi}\gamma^\mu\partial_\mu - (\partial_\mu\overline{\psi})\gamma^\mu\big)\psi - M\overline{\psi}\psi - g\phi\overline{\psi}\psi - \lambda\phi^4 \right]. \tag{2.1}$$

For the problem of interest here, the $\lambda\phi^4$ interaction will not be needed. The operator P^- which controls the dynamics is

$$P^- = \frac{1}{2}\int dx^- d^2x\; T^{+-}\,, \tag{2.2}$$

where

$$\begin{aligned} T^{+-} \;=\; & (\boldsymbol{\partial}_\perp\phi)^2 + \mu^2\phi^2 - i\psi_-^\dagger(\partial^+\psi_-) \\ & +2\psi_-^\dagger\gamma^0(-i\gamma^i\partial_i + M + g\phi)\psi_+ + \text{h.c.} \end{aligned} \tag{2.3}$$

The field ψ_- is nondynamical and can be eliminated via the constraint relation

$$i\partial_-\psi_- = \frac{1}{2}\gamma^0\big[-i\gamma^i\partial_i + M + g\phi\big]\psi_+. \tag{2.4}$$

For the second order shift in the eigenvalue of the operator P^- of the one-fermion state with $\boldsymbol{p}_\perp = 0$, one easily calculates

$$\frac{\alpha}{2\pi^2}\int_0^1 \frac{dx}{1-x}\int d^2q_\perp \frac{\boldsymbol{q}_\perp^2 + (2-x)^2M^2}{\boldsymbol{q}_\perp^2 + x^2M^2 + (1-x)\mu^2}\,, \tag{2.5}$$

where

$$\alpha \equiv \frac{g^2}{4\pi}\,. \tag{2.6}$$

The integral is divergent in the ultraviolet and must be regulated. Let us first consider regulating the integral with a momentum cutoff. While several possibilities might be considered, including a cutoff on $\boldsymbol{q}_\perp$ alone, the most commonly used cutoffs couple q^+ and $\boldsymbol{q}_\perp$ in some way. To retain boost invariance we will consider the "invariant mass" cutoff in which the total invariant mass of the intermediate state is limited [10]. For the present case this rule gives

$$\frac{q_\perp^2 + \mu^2}{x} + \frac{q_\perp^2 + M^2}{1-x} \le \Lambda^2\,. \tag{2.7}$$

This cutoff also appears if we simply limit the change in mass of the matrix elements of the interaction Hamiltonian. For the integral we then get

$$I(\mu^2, M^2, \Lambda^2) \equiv \frac{\alpha}{2\pi^2} \int_{L_-}^{L_+} \frac{dx}{1-x} \int_{\boldsymbol{q}_\perp^2 \le L} d^2q_\perp \frac{\boldsymbol{q}_\perp^2 + (2-x)^2 M^2}{\boldsymbol{q}_\perp^2 + x^2 M^2 + (1-x)\mu^2}\,, \tag{2.8}$$

where

$$\begin{aligned} L_\pm &= \frac{1}{2\Lambda^2}\left[\Lambda^2 + \mu^2 - M^2 \pm \sqrt{(\Lambda^2 + \mu^2 - M^2)^2 - 4\Lambda^2\mu^2}\right]\,, \\ L &= \Lambda^2 x(1-x) - \mu^2(1-x) - M^2 x\,. \end{aligned} \tag{2.9}$$

The integral can be done in closed form, but the result for arbitrary parameters is not terribly illuminating. If we take $\Lambda^2 \gg \mu^2 \gg M^2$ we get

$$\begin{aligned} I(\mu^2, M^2, \Lambda^2) \approx \frac{\alpha}{2\pi}\Bigg[&\left(\frac{\Lambda^2}{2} - \mu^2 \ln\Lambda^2 + \mu^2 \ln\mu^2 - \frac{\mu^4}{2\Lambda^2}\right) \\ &+ M^2\left(3\ln\Lambda^2 - 3\ln\mu^2 - \frac{9}{2} + \frac{5\mu^2}{\Lambda^2}\right) \\ &+ M^4\left(\frac{2}{\mu^2}\ln(M^2/\mu^2) + \frac{1}{3\mu^2} - \frac{1}{2\Lambda^2}\right)\Bigg]\,. \end{aligned} \tag{2.10}$$

Perhaps the most striking thing about this result is not so much that it is quadratically divergent as $\Lambda \to \infty$, but that it does not go to zero with M. This is in contrast to the Feynman result. In fact the vanishing of the self mass with vanishing bare mass is formally protected by the discrete chiral symmetry: $\psi \to i\gamma_5\psi$, with $\phi \to -\phi$. That I is not proportional to M^2 is due to the fact that the invariant mass regulator does not preserve this symmetry.

It is well known that the four-dimensional Feynman integral for the fermion self energy can be regulated by the addition of one Pauli–Villars boson field. If that is done the integral is then "finite" by power counting and vanishes with M. One might then think that if one first performs the q^- integral one would get a finite three-dimensional light-cone integral. However, the Feynman integral is only conditionally convergent, and therefore any value ascribed to it is a prescription. The standard integration procedure - symmetric integration in the spatial momenta with the q^0 integral done last - preserves the discrete chiral symmetry and thus leads to the vanishing of the result at $M = 0$. The terms in (2.10) which do not vanish as $M \to 0$ at large Λ include terms quadratic in Λ, logarithmic in Λ, and independent of Λ. Therefore three Pauli–Villars bosonic fields are necessary to render the light-cone integral consistent with discrete chiral symmetry. The entire light-cone integral (2.10) is then finite and vanishes as $M \to 0$. Thus we need three Pauli–Villars conditions:

$$\alpha + \sum_{i=1}^{3}\alpha_i = 0\,, \quad \alpha\mu^2 + \sum_{i=1}^{3}\alpha_i\mu_i^2 = 0\,, \quad \sum_{i=1}^{3}\alpha_i\mu_i^2\ln(\mu_i^2/\mu^2) = 0\,, \tag{2.11}$$

where the α_i's and μ_i's are the coupling constants and masses of the heavy fields. The logarithmic divergent term $3M^2\ln\Lambda^2$ in (2.10) returns if the masses of the heavy fields go to infinity, but the nonzero value at $M = 0$ does not return. The fact that three Pauli–Villars fields are necessary to regulate the self-energy graph in the light-cone representation is an old result [11], and it has received considerable study in [12]. One might wonder whether

there is some feature of the theory from a purely equal-time perspective that would allow one to predict the number of heavy fields necessary to regulate the calculation in the light-cone representation.[1]

To perform a DLCQ calculation one must limit the range of the momenta (which the Λ cutoff does) as well as make the momenta discrete by introducing periodicity conditions for the fields on the surface $x^+ = 0$. We may take $\psi_+ = \Lambda_+\psi$ to be antiperiodic in x^- and periodic in $\boldsymbol{x}_\perp$. (See Appendix A.) The scalar fields are taken to be periodic in both x^- and $\boldsymbol{x}_\perp$. With the heavy fields and the momentum cutoff in place, the only effect of the periodicity conditions on the above perturbation calculation is that the finite integral is then evaluated as a discrete sum. The convergence of the discrete sum to the continuum result is discussed below.

The discussion in this section suggests a new general procedure for resolution of the UV divergences of light-cone Hamiltonian field theory. The heavy fields will produce the counterterms necessary to make a consistent renormalization possible. What we propose is to test this procedure nonperturbatively, that is, include enough heavy fields in the Lagrangian to regulate perturbation theory, then produce a finite matrix with a momentum cutoff and discretization. The periodicity conditions can also lead to constrained zero modes, as discussed in [14]. Another important advantage of the Pauli–Villars fields is that the terms from the constrained zero modes which would affect the one loop mass shift (the most singular terms due to the constrained zero modes) are zero at the level of P^-. In the present paper we shall not attempt a full Yukawa calculation. We shall illustrate the method for a soluble model and provide some discussion of numerical issues.

B. Discrete Evaluation of the Light-Cone Integral

1. DLCQ

From the periodicity conditions in the light-cone box

$$-L < x^- < L\,, \quad -L_\perp < x, y < L_\perp\,, \tag{2.12}$$

one obtains discrete momenta

$$p^+ \to \frac{\pi}{L} n\,, \quad \boldsymbol{p}_\perp \to (\frac{\pi}{L_\perp} n_x, \frac{\pi}{L_\perp} n_y)\,, \tag{2.13}$$

with n even for bosons and odd for fermions. Integrals are then replaced by discrete sums obtained as trapezoidal approximations on the grid of momentum values

$$\int dp^+ \int d^2p_\perp f(p^+, \boldsymbol{p}_\perp) \simeq \frac{2\pi}{L} \left(\frac{\pi}{L_\perp}\right)^2 \sum_n \sum_{n_x, n_y = -N_\perp}^{N_\perp} f(n\pi/L, \boldsymbol{n}_\perp \pi/L_\perp)\,. \tag{2.14}$$

---

[1] We are not certain, but we speculate that it may be the same number necessary to regulate time-ordered perturbation theory in the equal-time representation; perhaps the results of [13] on the connection between the two representations could then be extended to higher order.

The limit $L \to \infty$ can be exchanged for a limit in terms of the integer *resolution* [1] $K \equiv \frac{L}{\pi} P^+$. The longitudinal momentum fraction $x = p^+/P^+$ becomes n/K. $H_{\rm LC}$ is independent of L.

Because the longitudinal integers n are always positive, DLCQ automatically limits the number of particles to no more than $\sim K/2$. The integers n_x and n_y range between limits associated with some maximum integer $N_\perp$ fixed by $L_\perp$ and a cutoff that limits transverse momentum.

The momentum-space continuum limit is reached when K and $N_\perp$ become infinite. The transverse length scale $L_\perp$ is chosen such that $N_\perp \pi / L_\perp$ is the largest transverse momentum allowed by the cutoff. The integrations for Pauli–Villars subtractions use the transverse scale $L_\perp$ determined for the physical boson. This insures use of a common grid that can easily represent momentum conservation in interactions.

We then compute the dimensionless integral

$$\tilde{I}(\mu^2, M^2, \Lambda^2) \equiv \frac{2\pi^2}{\alpha \mu^2} I(\mu^2, M^2, \Lambda^2) \tag{2.15}$$

and the subtracted integral

$$\tilde{I}_{\rm sub}(M^2/\mu^2, \mu_i^2/\mu^2, \Lambda^2/\mu^2) \equiv \tilde{I}(\mu^2, M^2, \Lambda^2) + \sum_i \frac{\alpha_i}{\alpha} \tilde{I}(\mu_i^2, M^2, \Lambda^2)\,. \tag{2.16}$$

When the loop integrals are evaluated numerically, the proportion of error increases with each subtraction. Once all three Pauli–Villars subtractions are done, the error can dominate. This is the case for an ordinary DLCQ calculation. The individual integrals are large and therefore must be computed accurately for the differences to be accurate. It can be helpful to have well separated Pauli–Villars masses, because the coefficients α_i are then $\mathcal{O}(1)$ and do not amplify the errors.

The domain of integration, as defined by the invariant-mass cutoff, is not commensurate with the DLCQ grid. This causes errors of two types: one is a truncation error where the edge of the domain is not properly counted and the other is the loss of rotational symmetry in the transverse grid. In one-dimensional cases, only the former type occurs. In that context, it is easily handled as part of an extrapolation in K; in the context of the three iterated integrals used for three dimensions, the error becomes much less controlled.

If the trapezoidal rule is applied to each iterated integral, as is done in the standard DLCQ approach, the errors will not follow a systematic dependence on the grid spacings for a reasonable number of grid points. This lack of systematic dependence on K and $N_\perp$ can be seen in Fig. 1.

These errors could be overcome with a commensurate grid that uses polar coordinates in the transverse direction. This would not be easily extended to situations with more than two particles. Also, it turns out that although a commensurate grid controls the errors in a systematic way, the errors are still large. Other methods that use the DLCQ grid have been found superior.

Given the rectangular DLCQ grid, one can improve on the simple application of the trapezoidal rule used in (2.14). The alternative integration schemes [15] are of the general form

$$\int d^n r\, f(\boldsymbol{r}) \simeq \sum_{i,j,\ldots} w_{i,j,\ldots} f(\boldsymbol{r}_{i,j,\ldots})\,, \tag{2.17}$$

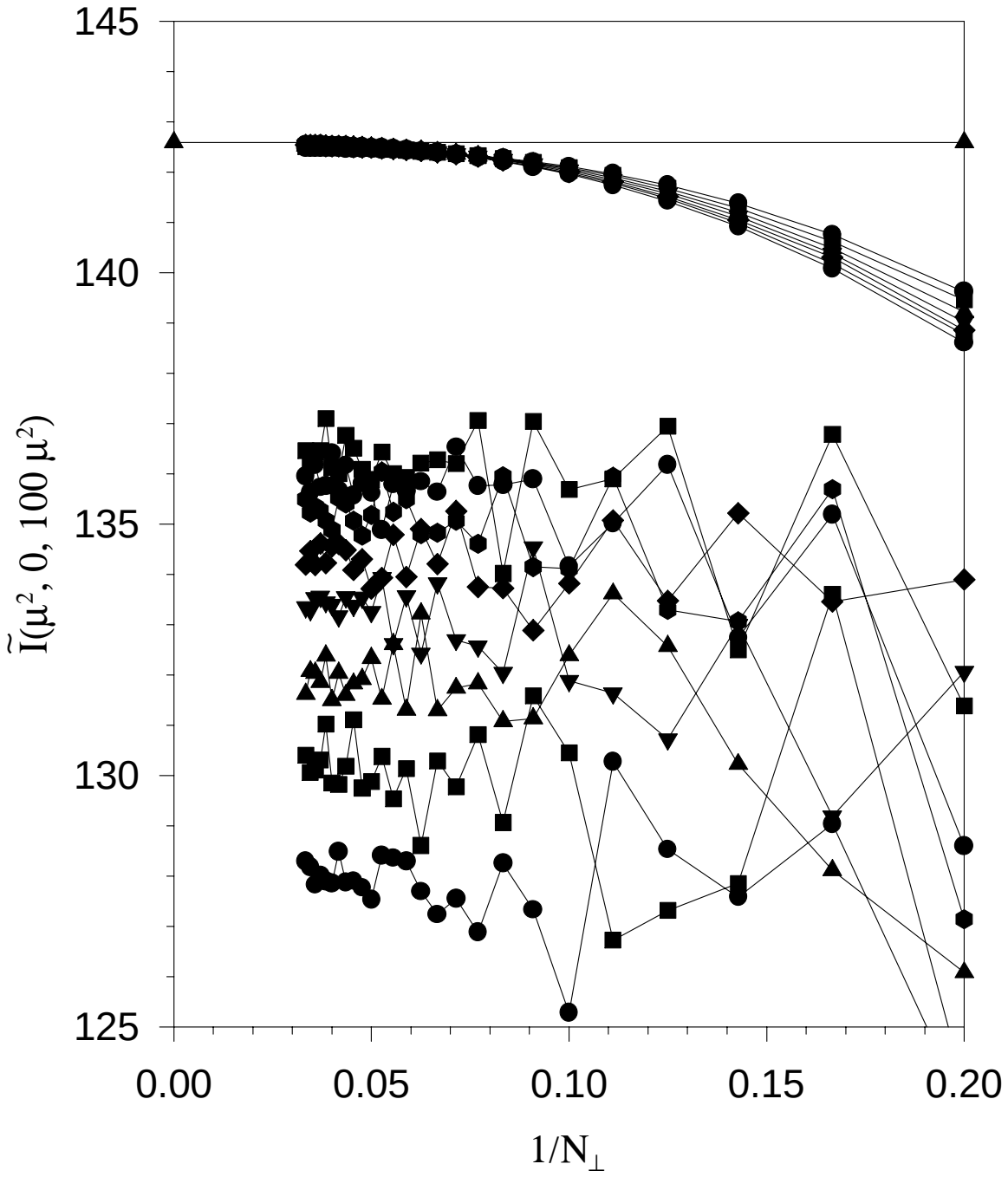

FIG. 1. One-loop fermion self energy. The horizontal line is the exact result. The smoothly curved results come from use of transverse circular weighting and longitudinal Simpson weighting. The scattered results are from ordinary DLCQ calculations. The DLCQ grid parameters take the ranges $K = 10, 12, \ldots, 24$ and $N_\perp = 5, 6, \ldots, 30$. The lines connect points calculated with the same K value.

TABLE I. Values of the subtracted integral $\tilde{I}_{\rm sub}(M^2/\mu^2, \mu_i^2/\mu^2, \Lambda^2/\mu^2)$ in the limit of infinite cutoff. The Pauli–Villars masses are $\mu_1^2 = 10\mu^2$, $\mu_2^2 = 50\mu^2$ and $\mu_3^2 = 100\mu^2$.

M^2:	0	$0.01\mu^2$	$0.05\mu^2$	$0.1\mu^2$	$0.2\mu^2$
DLCQ, improved and extrapolated:	-0.064	0.11	0.70	1.37	2.70
Exact, to order M^4 and $M^4 \ln M^2$:	0.0	0.1402	0.6661	1.2721	2.3778

where, unlike the case of the trapezoidal rule, the weights $w_{i,j,\ldots}$ will not all be equal. Special formulas for intervals near the edge can be derived, and one can even consider variations on the higher-order Simpson's rule. The transverse integrations can be treated in polar coordinates with a basis of circles of irregular radii chosen to pass through the points of the square grid. These methods provide results for integrals far better than ordinary DLCQ, as shown in Fig. 1. A discussion of the details is given in Appendix B.

2. Results

The results for the momentum-space continuum limit of the discrete sums are obtained by extrapolations which use values of 20, 22, and 24 for K and 25 through 30 for $N_\perp$. All results are given in units of the boson mass μ. These are fit by least squares to either $c_0 + a_1/K^3 + b_1/N_\perp^2$ or $c_0 + a_1/K^3 + a_2/K^4 + b_1/N_\perp^2 + b_2/N_\perp^3$. The latter is used for the μ_1 integral. This means that at most 5 parameters are used in fits to 18 points.

Extrapolation to the continuum after subtraction is not as accurate as extrapolation of each integral separately. The subtraction of the discrete sums induces a greater variation in errors that is harder to fit properly.

The range in $N_\perp$ was selected to avoid values where the μ_2 integral was badly approximated. However, here "badly" is to be interpreted relative to the desired final error of 0.02, which is slightly more that 0.2% of the answer.

Values of the subtracted integral for different fermion masses M are plotted as functions of $1/\Lambda^2$ in Fig. 2. The extrapolation to $\Lambda = \infty$ can be done by fits to $I_\infty + a/\Lambda^2$. They yield the values in Table I. In obtaining these values, the error in each individual integral has been reduced to ± 0.02 as measured against the analytic result at $M^2 = 0$. This implies an error of ± 0.04 in the subtracted result. Extrapolation in Λ^2 induces additional uncertainty reflected in the miss by 0.06 of zero for $M^2 = 0$. The ratios of the tabulated values are correct to within error estimates. The result for the subtracted integral is roughly proportional to M^2, but for M^2 near $0.2\mu^2$ or larger, terms even beyond M^4 appear important.

The range of Λ^2 values used in the fits was from $155\mu^2$ to $200\mu^2$ in steps of $5\mu^2$. For $\Lambda^2 \le 150\mu^2$ there is some distortion. For $\Lambda^2 \le 120\mu^2$ there is significant distortion, largely due to the μ_3 integral, which is badly approximated by the few points that satisfy the cutoff.

The number of Fock states required for Pauli–Villars particles is approximately 1.5 times the number for physical states. A listing of counts for two cases is given in Table II. Making μ_1 larger does decrease the number of Pauli–Villars states but this increases the coefficients α_i and thereby amplifies errors in the integrals. Also, with fewer states, the integrals themselves are approximated less accurately.

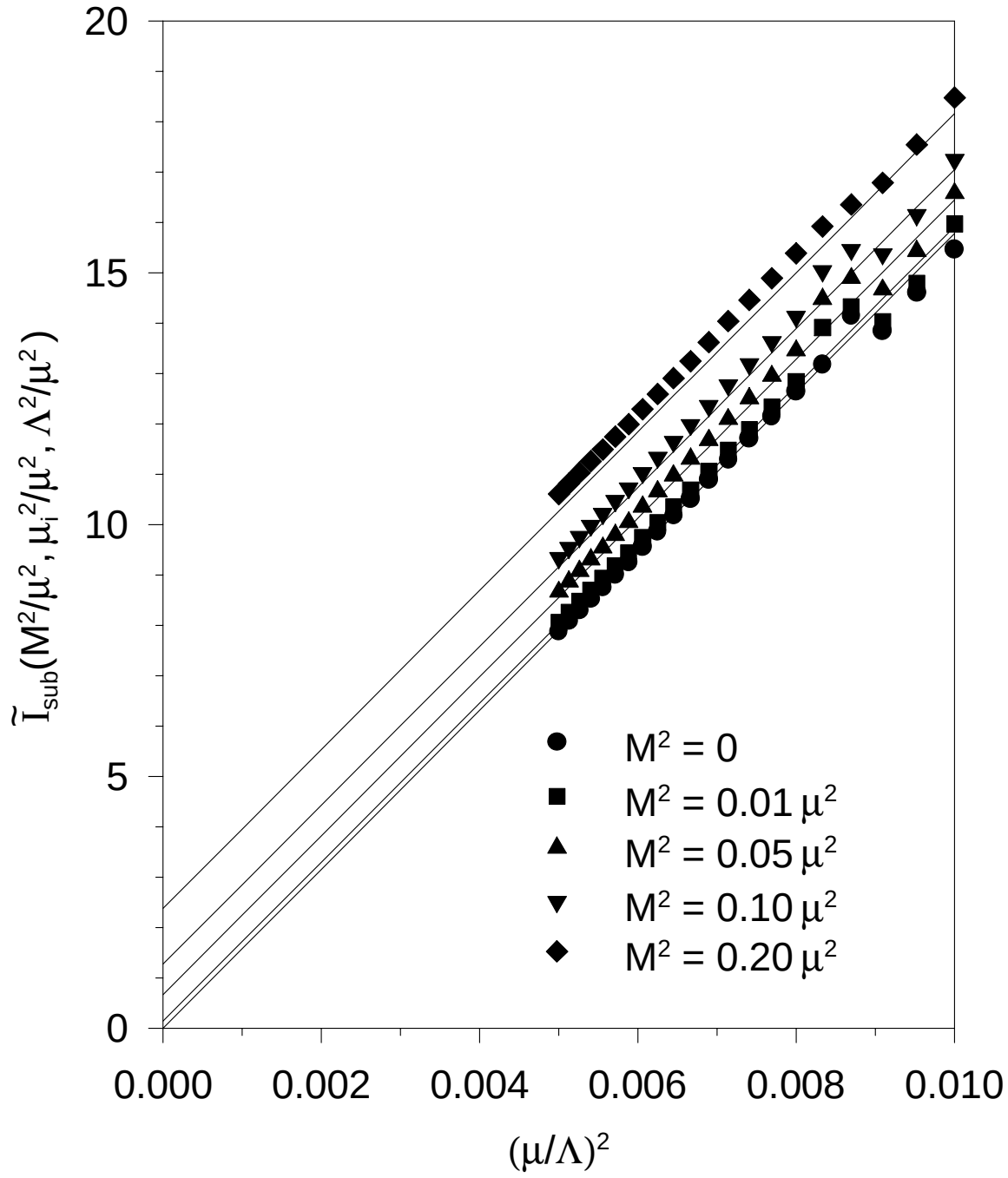

FIG. 2. Subtracted one-loop fermion self energy. The Pauli–Villars masses are $\mu_1^2 = 10\mu^2$, $\mu_2^2 = 50\mu^2$, and $\mu_3^2 = 100\mu^2$. The solid lines are from an analytic expansion in M^2 given in (2.10) of the text; additional terms are needed for $M^2 \gtrsim 0.2\mu^2$.

TABLE II. Number of Fock states used in two typical cases.

				Pauli–Villars			
Λ^2	K	$N_\perp$	physical	$\mu_1^2 = 10\mu^2$	$\mu_2^2 = 50\mu^2$	$\mu_3^2 = 100\mu^2$	total
200 μ^2	20	25	25975	22602	11142	3305	37049
200 μ^2	24	30	44943	39162	19293	5695	64150

III. A SOLUBLE MODEL

We now turn to the consideration of a nonperturbative problem.

A. The effective Hamiltonian

An effective Hamiltonian of the sort investigated by Greenberg and Schweber [9] and by Głazek and Perry [16] can be obtained from the Yukawa Hamiltonian [14] by modifying the momentum dependence in the fermion kinetic energy, $(M^2+p_\perp^2)/p^+ \longrightarrow (M_0^2+M_0'p^+)/P^+$, and by keeping only the no-flip three-point vertex in a modified form where the longitudinal momentum dependence is simplified. The fermion kinetic term in the Hamiltonian has a structure similar to that of the self-induced inertia term shown in Eq. (C.2) of Ref. [14]. This is a generalization of a static source. We include one Pauli–Villars field, which will prove sufficient in this case. The resulting light-cone Hamiltonian $H_{\rm LC}^{\rm eff} = P^+P_{\rm eff}^-$ is given by

$$\begin{aligned} H_{\rm LC}^{\rm eff} &= \int \frac{dp^+d^2p_\perp}{16\pi^3p^+}(M_0^2+M_0'p^+)\sum_\sigma b_{\underline{p}\sigma}^\dagger b_{\underline{p}\sigma} \\ &+ P^+\int\frac{dq^+d^2q_\perp}{16\pi^3q^+}\left[\frac{\mu^2+q_\perp^2}{q^+}a_{\underline{q}}^\dagger a_{\underline{q}}+\frac{\mu_1^2+q_\perp^2}{q^+}a_{1\underline{q}}^\dagger a_{1\underline{q}}\right] \\ &+ g\int\frac{dp_1^+d^2p_{\perp1}}{\sqrt{16\pi^3p_1^+}}\int\frac{dp_2^+d^2p_{\perp2}}{\sqrt{16\pi^3p_2^+}}\int\frac{dq^+d^2q_\perp}{16\pi^3q^+}\sum_\sigma b_{\underline{p}_1\sigma}^\dagger b_{\underline{p}_2\sigma} \\ &\quad\times\left[\left(\frac{p_1^+}{p_2^+}\right)^\gamma a_{\underline{q}}^\dagger\delta(\underline{p}_1-\underline{p}_2+\underline{q})+\left(\frac{p_2^+}{p_1^+}\right)^\gamma a_{\underline{q}}\delta(\underline{p}_1-\underline{p}_2-\underline{q})\right. \\ &\quad\left.+i\left(\frac{p_1^+}{p_2^+}\right)^\gamma a_{1\underline{q}}^\dagger\delta(\underline{p}_1-\underline{p}_2+\underline{q})+i\left(\frac{p_2^+}{p_1^+}\right)^\gamma a_{1\underline{q}}\delta(\underline{p}_1-\underline{p}_2-\underline{q})\right], \end{aligned} \tag{3.1}$$

with $\underline{p}\equiv(p^+,\boldsymbol{p}_\perp)$ and

$$\begin{aligned} \left[a_{\underline{q}},a_{\underline{q}'}^\dagger\right] &= 16\pi^3q^+\delta(\underline{q}-\underline{q}')\,, \\ \left\{b_{\underline{p}\sigma},b_{\underline{p}'\sigma'}^\dagger\right\} &= 16\pi^3p^+\delta(\underline{p}-\underline{p}')\delta_{\sigma\sigma'}\,. \end{aligned} \tag{3.2}$$

The Fock-state expansion of an eigenvector is

$$\begin{aligned} \Phi_\sigma = \sqrt{16\pi^3P^+}\sum_{n,n_1}\int\frac{dp^+d^2p_\perp}{\sqrt{16\pi^3p^+}}\prod_{i=1}^n\int\frac{dq_i^+d^2q_{\perp i}}{\sqrt{16\pi^3q_i^+}}\prod_{j=1}^{n_1}\int\frac{dr_j^+d^2r_{\perp j}}{\sqrt{16\pi^3r_j^+}} \\ \times\delta(\underline{P}-\underline{p}-\sum_i^n\underline{q}_i-\sum_j^{n_1}\underline{r}_j)\phi^{(n,n_1)}(\underline{q}_i,\underline{r}_j;\underline{p})\frac{1}{\sqrt{n!n_1!}}b_{\underline{p}\sigma}^\dagger\prod_i^n a_{\underline{q}_i}^\dagger\prod_j^{n_1}a_{1\underline{r}_j}^\dagger|0\rangle\,. \end{aligned} \tag{3.3}$$

The normalization condition for this state is

$$\Phi'^{\dagger}_{\sigma} \cdot \Phi_{\sigma} = 16\pi^3 P^+ \delta(\underline{P}' - \underline{P}) \,, \tag{3.4}$$

which yields the following condition on the individual amplitudes:

$$1 = \sum_{n,n_1} \prod_i^n \int dq_i^+ d^2q_{\perp i} \prod_j^{n_1} \int dr_j^+ d^2 r_{\perp j} \left| \phi^{(n,n_1)}(\underline{q}_i, \underline{r}_j; \underline{P} - \sum_i \underline{q}_i - \sum_j \underline{r}_j) \right|^2 . \tag{3.5}$$

B. Analytic solution

We seek a solution to

$$H^{\rm eff}_{\rm LC} \Phi_\sigma = M^2 \Phi_\sigma \,. \tag{3.6}$$

With $y_i = q_i^+/P^+$ and $z_j = r_j^+/P^+$, the amplitudes must then satisfy

$$\begin{aligned}
&\left[M^2 - M_0^2 - M_0' p^+ - \sum_i \frac{\mu^2 + q_{\perp i}^2}{y_i} - \sum_j \frac{\mu_1^2 + r_{\perp j}^2}{z_j} \right] \phi^{(n,n_1)}(\underline{q}_i, \underline{r}_j, \underline{p}) \\
&\quad = g \Bigg\{ \sqrt{n+1} \int \frac{dq^+ d^2 q_\perp}{\sqrt{16\pi^3 q^+}} \left(\frac{p^+ - q^+}{p^+} \right)^\gamma \phi^{(n+1,n_1)}(\underline{q}_i, \underline{q}, \underline{r}_j, \underline{p} - \underline{q}) \\
&\qquad + \frac{1}{\sqrt{n}} \sum_i \frac{1}{\sqrt{16\pi^3 q_i^+}} \left(\frac{p^+}{p^+ + q_i^+} \right)^\gamma \phi^{(n-1,n_1)}(\underline{q}_1, \ldots, \underline{q}_{i-1}, \underline{q}_{i+1}, \ldots, \underline{q}_n, \underline{r}_j, \underline{p} + \underline{q}_i) \\
&\qquad + i\sqrt{n_1 + 1} \int \frac{dr^+ d^2 r_\perp}{\sqrt{16\pi^3 r^+}} \left(\frac{p^+ - r^+}{r^+} \right)^\gamma \phi^{(n,n_1+1)}(\underline{q}_i, \underline{r}_j, \underline{r}, \underline{p} - \underline{r}) \\
&\qquad + \frac{i}{\sqrt{n_1}} \sum_j \frac{1}{\sqrt{16\pi^3 r_j^+}} \left(\frac{p^+}{p^+ + r_j^+} \right)^\gamma \phi^{(n,n_1-1)}(\underline{q}_i, \underline{r}_1, \ldots, \underline{r}_{j-1}, \underline{r}_{j+1}, \ldots, \underline{r}_{n_1}, \underline{p} + \underline{r}_j) \Bigg\} \,.
\end{aligned} \tag{3.7}$$

By construction, this coupled set of integral equations is identical in basic form to the equations considered by Greenberg and Schweber [9]. Their factorized *ansatz* for a solution suggests that we try

$$\phi^{(n,n_1)} = \sqrt{Z} \frac{(-g)^n (-ig)^{n_1}}{\sqrt{n! n_1!}} \left(\frac{p^+}{P^+} \right)^\gamma \prod_i \frac{y_i}{\sqrt{16\pi^3 q_i^+}(\mu^2 + q_{\perp i}^2)} \prod_j \frac{z_j}{\sqrt{16\pi^3 r_j^+}(\mu_1^2 + r_{\perp j}^2)} \,. \tag{3.8}$$

This is indeed a solution, provided that $M_0 = M$ and

$$M_0' = \frac{g^2/P^+}{16\pi^2} \frac{\ln \mu_1/\mu}{\gamma + 1/2} \,. \tag{3.9}$$

Although γ can be assigned any of a range of values, 1/2 is the natural choice, and we will use this value for the remainder of the paper. With this choice, the one-boson amplitude is proportional to $\sqrt{y(1-y)}$.

The normalization condition (3.5) implies

$$\frac{1}{Z} = \sum_{n,n_1} \frac{1}{(2n+2n_1+1)!n!n_1!} \frac{(g/\mu)^{2n}(g/\mu_1)^{2n_1}}{(16\pi^2)^{n+n_1}} \,. \tag{3.10}$$

Thus we can fix the bare mass and the wave function renormalization. However, there remains the bare coupling.[2]

C. Coupling renormalization

To fix the coupling we use $\langle :\phi^2(0):\rangle \equiv \Phi_\sigma^\dagger : \phi^2(0) : \Phi_\sigma$. For the analytic solution this expectation value reduces to

$$\langle :\phi^2(0):\rangle = \sum_{n,n_1} \frac{2Zn}{(2n+2n_1)!n!n_1!} \frac{(g/\mu)^{2n}(g/\mu_1)^{2n_1}}{(16\pi^2)^{n+n_1}} \,. \tag{3.11}$$

From a numerical solution it can be computed fairly efficiently in a sum similar to the normalization sum

$$\begin{aligned} \langle :\phi^2(0):\rangle = \sum_{n=1,n_1=0} \prod_i^n \int dq_i^+ d^2q_{\perp i} \prod_j^{n_1} \int dr_j^+ d^2 r_{\perp j} \left(\sum_{k=1}^n \frac{2}{q_k^+/P^+} \right) \\ \times \left| \phi^{(n,n_1)}(\underline{q}_i, \underline{r}_j; \underline{P} - \sum_i \underline{q}_i - \sum_j \underline{r}_j) \right|^2 \,. \end{aligned} \tag{3.12}$$

With the bare parameters determined, we "predict" a value for the slope of the fermion no-flip form factor. It is related to the transverse size of the dressed fermion. From [17] we find a useful expression for the form factor

$$\begin{aligned} F(Q^2) &= \frac{1}{2P^+} \langle P + p_\gamma \uparrow | J^+(0) | P \uparrow \rangle \\ &= \sum_j e_j \int 16\pi^3 \delta(1 - \sum_i x_i) \delta(\sum_i \boldsymbol{k}_{\perp i}) \prod_i \frac{dx_i d^2 p_{\perp i}}{16\pi^3} \psi^*_{P+p_\gamma\uparrow}(x_i, \boldsymbol{p}'_{\perp i}) \psi_{P\uparrow}(x_i, \boldsymbol{p}_{\perp i}) \,, \end{aligned} \tag{3.13}$$

where the matrix element has been evaluated in the frame with

$$P = (P^+, P^- = \frac{M^2}{P^+}, \boldsymbol{0}_\perp) \,, \quad p_\gamma = (0, p_\gamma^- = 2p_\gamma \cdot P/P^+, \boldsymbol{p}_{\gamma\perp}) \,, \quad Q^2 \equiv p_{\gamma\perp}^2 \,, \tag{3.14}$$

e_j is the charge of the jth constituent, and

$$\boldsymbol{p}'_{\perp i} = \begin{cases} \boldsymbol{p}_{\perp i} - x_i \boldsymbol{p}_{\gamma\perp} & i \neq j \\ \boldsymbol{p}_{\perp i} + (1-x_i)\boldsymbol{p}_{\gamma\perp} & i = j \,. \end{cases} \tag{3.15}$$

---

[2] In this model the bare coupling is finite.

A sum over Fock states is understood.

When the fermion is assigned a charge of 1, and the bosons remain neutral, the analytic solution yields

$$F(Q^2) = Z\sum_{n,n_1} \frac{(g^2/16\pi^3)^{n+n_1}}{n!n_1!} \int_0^1 \theta(1-\sum_i^n y_i - \sum_j^{n_1} z_j) \times \prod_i^n \frac{y_i dy_i d^2q_{\perp i}}{(\mu^2+q'^2_{\perp i})(\mu^2+q^2_{\perp i})} \prod_j^{n_1} \frac{z_j dz_j d^2r_{\perp j}}{(\mu^2+r'^2_{\perp j})(\mu^2+r^2_{\perp j})}\,, \tag{3.16}$$

with

$$\boldsymbol{q}'_\perp = \boldsymbol{q}_\perp - y\boldsymbol{p}_{\gamma\perp} \;\text{ and }\; \boldsymbol{r}'_\perp = \boldsymbol{r}_\perp - z\boldsymbol{p}_{\gamma\perp}\,. \tag{3.17}$$

The slope is extracted as

$$F'(0) = -\sum_{n,n_1} \frac{Z(n/\mu^2 + n_1/\mu_1^2)}{(2n+2n_1+3)!n!n_1!} \frac{(g/\mu)^{2n}(g/\mu_1)^{2n_1}}{(16\pi^2)^{n+n_1}}\,. \tag{3.18}$$

Numerically, one can compute $F'(0)$ from

$$F'(0) = \sum_{n,n_1} \prod_i^n \int dq_i^+ d^2q_{\perp i} \prod_j^{n_1} \int dr_j^+ d^2r_{\perp j} \times \left[\left(\sum_i \frac{y_i^2}{4}\nabla^2_{\perp i} + \sum_j \frac{z_j^2}{4}\nabla^2_{\perp j}\right)\phi^{(n,n_1)}(\underline{q}_i,\underline{r}_j;\underline{P}-\sum_i \underline{q}_i - \sum_j \underline{r}_j)\right]^* \times \phi^{(n,n_1)}(\underline{q}_i,\underline{r}_j;\underline{P}-\sum_i \underline{q}_i - \sum_j \underline{r}_j)\,, \tag{3.19}$$

with $\nabla^2_\perp$ represented by finite differences. It turns out that single derivatives of typical amplitudes can be better approximated than the double derivatives in the Laplacian. Integration by parts in (3.19) then leads to a computationally better quantity

$$\tilde{F}'(0) = -\sum_{n,n_1} \prod_i^n \int dq_i^+ d^2q_{\perp i} \prod_j^{n_1} \int dr_j^+ d^2r_{\perp j} \times \left[\sum_i \left|\frac{y_i}{2}\nabla_{\perp i}\phi^{(n,n_1)}(\underline{q}_i,\underline{r}_j;\underline{P}-\sum_i \underline{q}_i - \sum_j \underline{r}_j)\right|^2 + \sum_j \left|\frac{z_j}{2}\nabla_{\perp j}\phi^{(n,n_1)}(\underline{q}_i,\underline{r}_j;\underline{P}-\sum_i \underline{q}_i - \sum_j \underline{r}_j)\right|^2\right]\,, \tag{3.20}$$

which differs from $F'(0)$ by surface terms which vanish as $\Lambda \to \infty$.

D. Distribution functions

To further explore the wave functions $\phi^{(n,n_1)}$, we compute distribution functions for the constituent bosons

$$f_B(y) \equiv \sum_{n,n_1} \prod_i^n \int dq_i^+ d^2q_{\perp i} \prod_j^{n_1} \int dr_j^+ d^2r_{\perp j} \sum_{i=1}^{n} \delta(y - q_i^+/P^+) \times \left| \phi^{(n,n_1)}(\underline{q}_i, \underline{r}_j; \underline{P} - \sum_i \underline{q}_i - \sum_j \underline{r}_j) \right|^2 , \tag{3.21}$$

and the Pauli–Villars boson

$$f_{PV}(z) \equiv \sum_{n,n_1} \prod_i^n \int dq_i^+ d^2q_{\perp i} \prod_j^{n_1} \int dr_j^+ d^2r_{\perp j} \sum_{j=1}^{n_1} \delta(z - r_j^+/P^+) \times \left| \phi^{(n,n_1)}(\underline{q}_i, \underline{r}_j; \underline{P} - \sum_i \underline{q}_i - \sum_j \underline{r}_j) \right|^2 . \tag{3.22}$$

Their integrals yield the average multiplicities

$$\langle n_B \rangle = \int_0^1 f_B(y) dy \,, \quad \langle n_{PV} \rangle = \int_0^1 f_{PV}(z) dz \,. \tag{3.23}$$

For the analytic solution (3.8) we obtain

$$f_B(y) = \left(\frac{\mu_1}{\mu}\right)^2 f_{PV}(y) = \sum_{n,n_1} \frac{Zny(1-y)^{(2n+2n_1-1)}}{(2n+2n_1-1)!n!n_1!} \frac{(g/\mu)^{2n}(g/\mu_1)^{2n_1}}{(16\pi^2)^{n+n_1}} \,, \tag{3.24}$$

and

$$\langle n_B \rangle = \left(\frac{\mu_1}{\mu}\right)^2 \langle n_{PV} \rangle = \sum_{n,n_1} \frac{Zn}{(2n+2n_1+1)!n!n_1!} \frac{(g/\mu)^{2n}(g/\mu_1)^{2n_1}}{(16\pi^2)^{n+n_1}} \,. \tag{3.25}$$

For a numerical solution, the integrals can be approximated by sums.

IV. DLCQ APPLIED TO THE SOLUBLE MODEL

A. Discretization

The basic momentum discretization and approximation of integrals are discussed in Sec. II B 1. From these we construct discrete approximations to the eigenvector Φ_σ, the coupled equations (3.7) for the amplitudes, and the derived quantities $\langle :\phi^2(0):\rangle$, $\tilde{F}'$ and distribution amplitudes. Creation operators for discrete momenta are defined by

$$b^\dagger_{\underline{n}\sigma} = \frac{\pi/L_\perp}{\sqrt{8\pi^3 n}} b^\dagger_{\underline{p}\sigma} \,, \quad a^\dagger_{\underline{m}} = \frac{\pi/L_\perp}{\sqrt{8\pi^3 m}} a^\dagger_{\underline{q}} \,, \tag{4.1}$$

such that they satisfy simple commutation relations

$$\left\{b_{\underline{n}\sigma}, b^\dagger_{\underline{n}\sigma}\right\} = \delta_{\underline{n}'\underline{n}}\delta_{\sigma'\sigma}\,, \quad \left[a_{\underline{n}}, a^\dagger_{\underline{n}}\right] = \delta_{\underline{n}'\underline{n}}\,. \tag{4.2}$$

These follow from (3.2) and the discrete delta-function representation

$$\delta(\underline{p}-\underline{p}') = \frac{L}{2\pi}\left(\frac{L_\perp}{\pi}\right)^2 \delta_{\underline{n}'\underline{n}}\,. \tag{4.3}$$

The discrete approximation of the eigenvectors is then

$$\begin{aligned}\tilde{\Phi}_\sigma \equiv \frac{\pi}{L_\perp}\Phi_\sigma = \sqrt{8\pi^3 K}\sum_{n,n_1}\sum_{\underline{n}}\prod_{i=1}^{n}\sum_{\underline{m}_i}\prod_{j=1}^{n_1}\sum_{\underline{l}_j}\delta_{\underline{K},\underline{n}+\sum_i^n \underline{m}_i+\sum_j^{n_1}\underline{l}_j} \\ \times\tilde{\phi}^{(n,n_1)}(\underline{m}_i,\underline{l}_j;\underline{n})\frac{1}{\sqrt{n!n_1!}}b^\dagger_{\underline{n}\sigma}\prod_i^n a^\dagger_{\underline{m}_i}\prod_j^{n_1}a^\dagger_{1\underline{l}_j}|0\rangle\,,\end{aligned}$$

where

$$\tilde{\phi}^{(n,n_1)} = \left[\frac{2\pi}{L}\left(\frac{\pi}{L_\perp}\right)^2\right]^{(n+n_1)/2}\phi^{(n,n_1)} \tag{4.4}$$

are rescaled amplitudes, for which the normalization condition (3.5) becomes

$$1 = \sum_{n,n_1}\prod_{i=1}^{n}\sum_{\underline{m}_i}\prod_{j=1}^{n_1}\sum_{\underline{l}_j}\left|\tilde{\phi}^{(n,n_1)}(\underline{m}_i,\underline{l}_j,\underline{K}-\sum_i\underline{m}_i-\sum_j\underline{l}_j)\right|^2\,. \tag{4.5}$$

The most convenient basis for a numerical calculation is the number basis (or oscillator basis), which eliminates summation over states that differ by only rearrangement of bosons of the same type. We define collections of sums with a prime $\prod_{i=1}^n\sum'_{\underline{m}_i}$ as being restricted to one ordering of the momenta and introduce factorials $N_{\{\underline{m}_i\}}\equiv N_{\underline{m}_1}!N_{\underline{m}_2}!\cdots$ where $N_{\underline{m}_1}$ is the number of times that $\underline{m}_1$ appears in the collection $\{\underline{m}_i\}$. The amplitudes for this number basis are

$$\psi^{(n,n_1)} = \sqrt{\frac{n!n_1!}{N_{\{\underline{m}_i\}}N_{\{\underline{l}_j\}}}}\tilde{\phi}^{(n,n_1)}\,, \tag{4.6}$$

with normalization

$$1 = \sum_{n,n_1}\prod_{i=1}^{n}\sum_{\underline{m}_i}{}'\prod_{j=1}^{n_1}\sum_{\underline{l}_j}{}'\left|\psi^{(n,n_1)}\right|^2\,. \tag{4.7}$$

In this basis the discretization of the coupled equations (3.7) yields

$$\left[\tilde{M}^2-\tilde{M}_0^2-\tilde{M}_0'\frac{n}{K}-\sum_i\frac{1+(m_{ix}^2+m_{iy}^2)/\tilde{L}_\perp^2}{m_i/K}-\sum_j\frac{\tilde{\mu}_1^2+(l_{jx}^2+l_{jy}^2)/\tilde{L}_\perp^2}{l_j/K}\right]\psi^{(n,n_1)}(\underline{m}_i,\underline{l}_j,\underline{n})$$

TABLE III. Basis sizes for DLCQ calculations in the soluble model with parameters $M^2 = \mu^2$, $\mu_1^2 = 10\mu^2$, and $\Lambda^2 = 50\mu^2$. The numbers of physical states are in parentheses.

	K							
$N_\perp$	3	5	7	9	11	13	15	17
1	3	8	18	38	36	65	110	185
	(2)	(4)	(7)	(12)	(19)	(30)	(45)	(67)
2	19	70	218	265	590	1120	822	1410
	(10)	(32)	(127)	(119)	(343)	(754)	(453)	(626)
3	43	222	958	1408	4460	17031	22486	21635
	(22)	(102)	(367)	(736)	(2671)	(9230)	(13213)	(13531)
4	75	872	3714	9259	49394	50966	110254	328966
	(38)	(330)	(1399)	(5913)	(32363)	(32124)	(55319)	(172247)
5	99	2028	13702	54100	95176	386140	1553576	
	(50)	(722)	(5699)	(28065)	(66371)	(232400)	(1038070)	
6	139	3982	35666	126748	536758	2907158		
	(70)	(1548)	(12991)	(69245)	(391511)	(2107688)		
7	195	7734	79794	519325	1317392			
	(98)	(2780)	(32891)	(276299)	(1008539)			
8	275	11736	172118	1165832				
	(138)	(4268)	(61947)	(687394)				

$$
\begin{aligned}
= \frac{g/\mu}{\tilde{L}_\perp \sqrt{8\pi^3}} \Bigg\{ & \sum_{\underline{m}} \frac{1}{\sqrt{m}} \sqrt{\frac{N_{\{\underline{m},\underline{m}_i\}}}{N_{\{\underline{m}_i\}}}} \left(\frac{n-m}{n}\right)^\gamma \psi^{(n+1,n_1)}(\underline{m}_i, \underline{m}, \underline{l}_j, \underline{n}-\underline{m}) \\
& + \sum_i \frac{1}{\sqrt{m_i}} \sqrt{\frac{N_{\{\underline{m}_i\}'}}{N_{\{\underline{m}_i\}}}} \left(\frac{n}{n+m_i}\right)^\gamma \psi^{(n-1,n_1)}(\underline{m}_1, \ldots, \underline{m}_{i-1}, \underline{m}_{i+1}, \ldots, \underline{m}_n, \underline{l}_j, \underline{n}+\underline{m}_i) \\
& + i \sum_{\underline{l}} \frac{1}{\sqrt{l}} \sqrt{\frac{N_{\{\underline{l},\underline{l}_j\}}}{N_{\{\underline{l}_j\}}}} \left(\frac{n-l}{n}\right)^\gamma \psi^{(n,n_1+1)}(\underline{m}_i, \underline{l}_j, \underline{l}, \underline{n}-\underline{l}) \\
& + i \sum_j \frac{1}{\sqrt{l_j}} \sqrt{\frac{N_{\{\underline{l}_j\}'}}{N_{\{\underline{l}_j\}}}} \left(\frac{n}{n+l_j}\right)^\gamma \psi^{(n,n_1-1)}(\underline{m}_i, \underline{l}_1, \ldots, \underline{l}_{j-1}, \underline{l}_{j+1}, \ldots, \underline{l}_{n_1}, \underline{n}+\underline{l}_j) \Bigg\} ,
\end{aligned}
\tag{4.8}
$$

where $\underline{n} = \underline{K} - \sum_i \underline{m}_i - \sum_j \underline{l}_j$, $\{\underline{m}_i\}'$ is the set of boson momenta without $\underline{m}_i$, and a tilde implies division by μ except for $\tilde{L}_\perp = \mu L_\perp/\pi$. This is a matrix eigenvalue problem, which for given g, μ, M, μ_1, and Λ we solve for ψ and M_0^2. The cutoff Λ^2 is applied as a limit on the invariant mass of individual particles, rather than on the total invariant mass of a Fock state. Typical basis sizes are given in Table III.

The bare coupling g is fixed by setting a value for

$$
\langle :\phi^2(0): \rangle \simeq \sum_{n,n_1} \prod_{i=1}^{n} \sum_{\underline{m}_i}{}' \prod_{j=1}^{n_1} \sum_{\underline{l}_j}{}' \sum_{k=1}^{n} \frac{2K}{m_k} \left|\psi^{(n,n_1)}\right|^2 . \tag{4.9}
$$

The combination of the matrix equation and the imposed constraint on $\langle :\phi^2(0): \rangle$ is solved

iteratively. The form factor slope $\tilde{F}'(0)$, the distribution functions, and average multiplicities are all approximated by similar discrete sums over the amplitudes $\psi^{(n,n_1)}$.

B. Numerical techniques

The matrix equation (4.8) is solved using the Lanczos algorithm [18] for complex symmetric matrices, which is a special case of the biorthogonal Lanczos algorithm [19,20]. Given an initial guess $\boldsymbol{u}_1$ for an eigenvector of a complex symmetric matrix A, a sequence of vectors $\{\boldsymbol{u}_n\}$ is generated by the following steps:

$$\begin{aligned} \boldsymbol{v}_{n+1} &= A\boldsymbol{u}_n - b_n\boldsymbol{u}_{n-1} \quad (\text{with } b_1 = 0) \\ a_n &= \boldsymbol{v}_{n+1}\cdot\boldsymbol{u}_n \\ \boldsymbol{v}'_{n+1} &= \boldsymbol{v}_{n+1} - a_n\boldsymbol{u}_n \\ b_{n+1} &= \sqrt{\boldsymbol{v}'_{n+1}\cdot\boldsymbol{v}'_{n+1}} \\ \boldsymbol{u}_{n+1} &= \boldsymbol{v}'_{n+1}/b_{n+1}\,. \end{aligned} \tag{4.10}$$

The dot products do not involve conjugation, and the constants a_n and b_n are in general complex. The process will fail if b_{n+1} is zero for nonzero $\boldsymbol{v}'_{n+1}$, which can happen in principle but does not seem to happen in practice [20]. If $\boldsymbol{v}'_{n+1}$ is zero, the process terminates naturally. The vectors $\boldsymbol{u}_{n-1}$, $\boldsymbol{v}_{n+1}$, $\boldsymbol{v}'_{n+1}$, and $\boldsymbol{u}_{n+1}$ can all be stored in the same array. At any one time only two vectors, one of these and $\boldsymbol{u}_n$, need to be kept.

The vectors $\boldsymbol{u}_n$ are orthogonal to each other, and the a_n and b_n form the diagonal and co-diagonal of a complex symmetric tridiagonal matrix which represents A in the basis $\{\boldsymbol{u}_n\}$. If the process has terminated with a $\boldsymbol{v}'_{n+1} = 0$ for some n, the tridiagonal representation is an exact representation for some subspace, and diagonalization yields some of the eigenvalues of A. If the process is terminated at some arbitrary early point, the eigenvalues of the tridiagonal matrix will approximate those of A. The approximation is particularly good for the extreme eigenvalues after only a few iterations. Depending on the initial guess, the number of iterations may need to be only 20, independent of the size of A. To reconstruct the eigenvectors of the original matrix, all of the $\boldsymbol{u}_n$ need to be kept. Because only two are needed in the Lanczos algorithm, the others can be written temporarily to disk and retrieved later.

We use the analytic solution (3.8) as the initial guess. Its components are either real or imaginary, and the process of matrix multiplication and division/multiplication by b_n preserves this structure in a controlled way. The diagonal elements a_n can be shown to be real and the off-diagonal elements b_n are either real or imaginary. This reduces the storage needed and eliminates the need for explicit complex arithmetic.

To further reduce storage requirements, we take full advantage of the transposition symmetry and sparsity of the matrix. Only nonzero elements and their indices are stored. The coupling g is factored out so that the matrix can be reused without change in the iterations that solve for g.

To improve convergence, we include weighting factors of the sort discussed in Sec. II B 1 and Appendix B. The circular form for transverse sums is used for two-body amplitudes and the extended trapezoidal rule is used for all others, with one exception. If the coefficients

(B2) for the extended trapezoidal rule become negative, a rectangle approximation is used. This is because restoration of symmetry for the weighted matrix requires the square roots of the weights. Schematically the symmetrization process is

$$\sum_j A_{ij} w_j u_j = \xi u_i \quad \longrightarrow \quad \sum_j \sqrt{w_i w_j} A_{ij} \sqrt{w_j} u_j = \xi \sqrt{w_i} u_i \,, \tag{4.11}$$

where $\sqrt{w_i w_j} A_{ij}$ is the new symmetric matrix.

The complete specification of the weighting factors requires selection of integration order, because the limits of integration are interrelated by the cutoff. The simplest reduction of these interrelationships is made if all sums in one transverse direction are done before those in the orthogonal transverse direction, and all of these before the longitudinal sums. Within each of these three groupings the sums are done for one particle at a time in the ordered momentum list. One consequence of this choice is that the transverse directions are treated asymmetrically (except for the two-body sectors). This induces a small transverse asymmetry in the amplitudes of the solution, including the two-body amplitudes. The asymmetry disappears in the numerical limit $N_\perp \to \infty$.

C. Results

We have solved the discrete eigenvalue problem (4.8) for various cases. The physical parameter values chosen were $\gamma = 1/2$, $M^2 = \mu^2$, $\mu_1^2 = 10\mu^2$, and $\langle :\phi^2(0):\rangle = 1$ or 2. The parameters that control the numerical approximation, namely Λ^2, K, and $N_\perp$ (or $L_\perp$), were varied to study convergence with basis sizes up to $\sim 520,000$. The ranges of these numerical parameters are shown in Tables IV and V. The transverse scale $L_\perp$ was chosen such that $N_\perp$ radial points satisfy the invariant-mass cutoff for one-boson states at the value of longitudinal momentum that yields maximum transverse width. The bare fermion mass M_0 was allowed to vary from its analytic, infinite-cutoff value of M in order that M could be held fixed. The tables list the values of M_0 along with those of the bare coupling g, as set by (4.9), the average boson multiplicity $\langle n_B\rangle$, and, for $\langle :\phi^2(0):\rangle = 1$, the slope $\tilde{F}'(0)$ of the fermion form factor. The analytic, infinite-cutoff values are also included.

The values of the form factor slope are very poor approximations. This is due to the sensitivity to $N_\perp$ of the finite difference representation of the derivatives in (3.20). A good approximation requires at least $N_\perp = 8$, which implies very large basis sizes even for small K.

The results for g and $\langle n_B\rangle$ are surprisingly insensitive to variation in K and $N_\perp$. Only the cutoff Λ^2 is important. This is mirrored in the distribution functions shown in Figs. 3-6. Again, variations in K and $N_\perp$ make little difference; however, one can see that the cutoff has an important effect. Smaller cutoffs produce an enhancement in the interval (0.4, 0.8).[3]

The amplitude for the one-boson state is shown in Fig. 7. The analytic result is shown for comparison. As can be seen, the two shapes are nearly identical.

---

[3]Recall that the distribution function does not have a fixed normalization but instead determines the average multiplicity, which is then also enhanced at finite cutoff.

TABLE IV. Numerical parameter values and results from solving the model eigenvalue problem. The physical parameter values were $M^2 = \mu^2$ for the fermion mass, $\mu_1^2 = 10\mu^2$ for the Pauli–Villars mass, and $\langle{:}\phi^2(0){:}\rangle = 1$ to fix the coupling g.

$(\Lambda/\mu)^2$	K	$N_\perp$	$\mu L_\perp/\pi$	$(M_0/\mu)^2$	g/μ	$\langle n_B\rangle$	$100\mu^2\tilde{F}'(0)$
50	11	4	0.8165	0.8547	13.293	0.177	-0.751
50	13	4	0.8165	0.8518	13.230	0.172	-1.015
50	15	4	0.8165	0.8408	13.556	0.178	-0.715
50	17	4	0.8165	0.8289	13.392	0.180	-0.565
50	9	5	1.2062	0.8601	14.023	0.179	-0.547
50	9	6	1.2247	0.8377	14.323	0.179	-0.582
50	9	7	1.4289	0.8302	14.386	0.179	-0.658
50	9	5	1.2062	0.8601	14.023	0.179	-0.547
100	9	5	0.7143	1.0520	12.565	0.174	-0.239
200	9	5	0.5025	1.1980	10.191	0.172	-0.139
∞		analytic		1.0000	13.148	0.160	-0.786

TABLE V. Same as Table IV except $\langle{:}\phi^2(0){:}\rangle = 2$.

$(\Lambda/\mu)^2$	K	$N_\perp$	$\mu L_\perp/\pi$	$(M_0/\mu)^2$	g/μ	$\langle n_B\rangle$
50	11	4	0.8165	0.5068	21.541	0.368
50	13	4	0.8165	0.5166	21.327	0.352
50	15	4	0.8165	0.4496	22.323	0.366
50	17	4	0.8165	0.4439	21.930	0.364
50	9	5	1.2062	0.5340	22.396	0.367
50	9	6	1.2247	0.5109	22.507	0.369
50	9	7	1.4289	0.5204	22.287	0.366
50	9	5	1.2062	0.5340	22.396	0.367
100	9	5	0.7143	0.9353	20.962	0.359
200	9	5	0.5025	1.3080	18.034	0.347
∞		analytic		1.0000	19.420	0.308

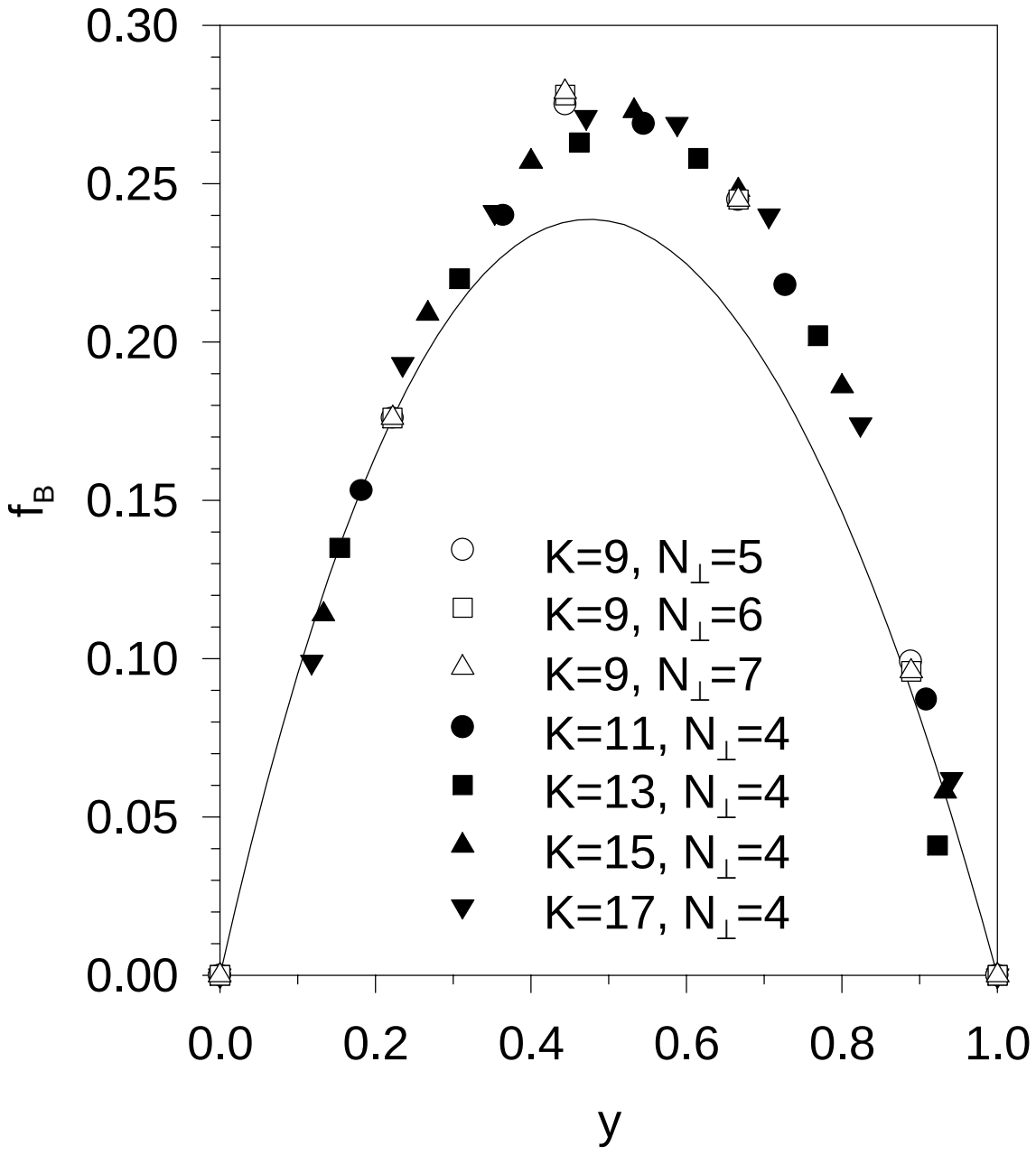

FIG. 3. The boson distribution function f_B at various numerical resolutions, with $\langle{:}\phi^2(0){:}\rangle = 1$ and $\Lambda^2 = 50\mu^2$. The solid line is the analytic result.

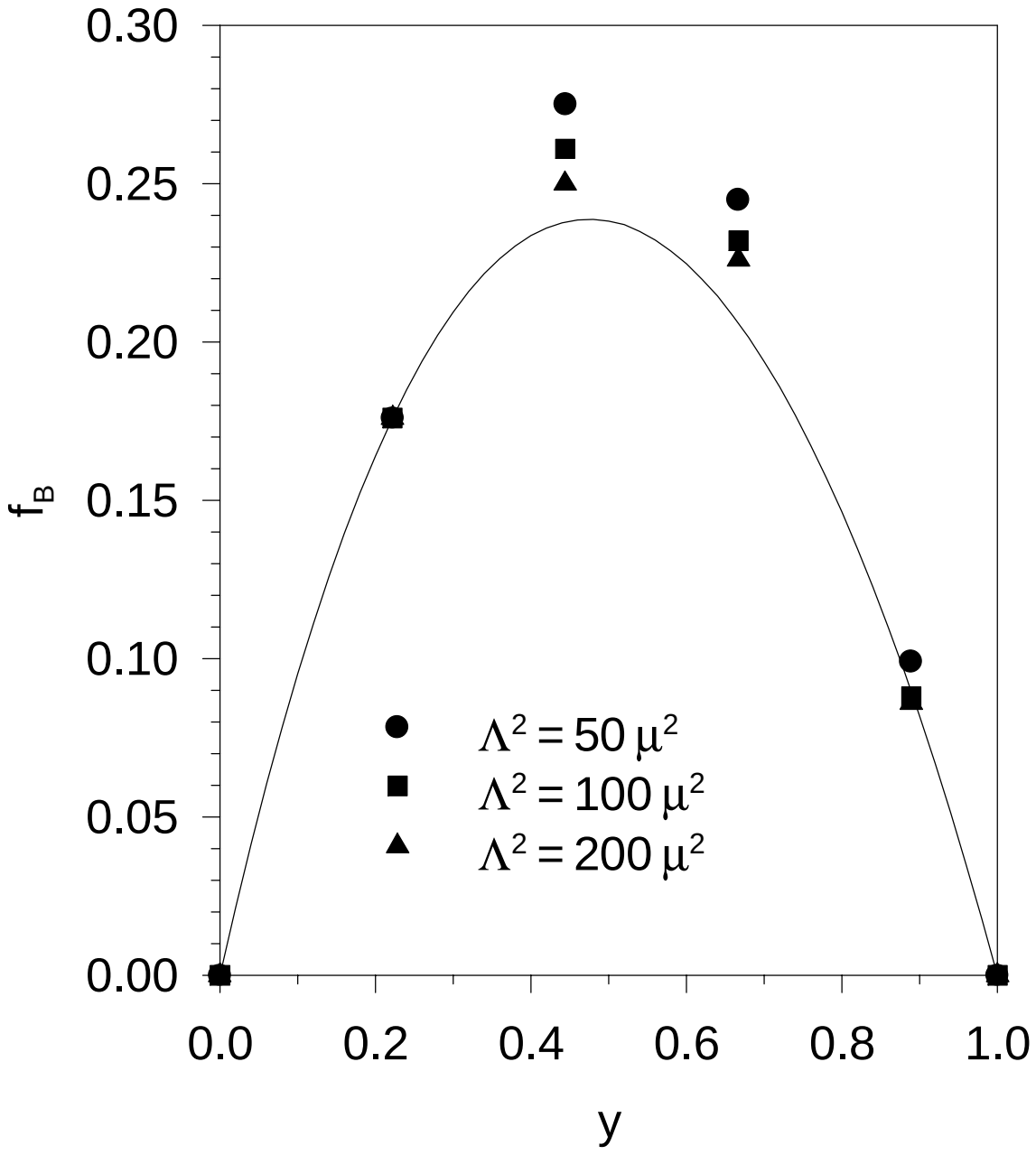

FIG. 4. The boson distribution function f_B for different cutoff values, with $\langle{:}\phi^2(0){:}\rangle = 1$ and numerical resolution set at $K = 9$ and $N_\perp = 5$. The solid line is the analytic result.

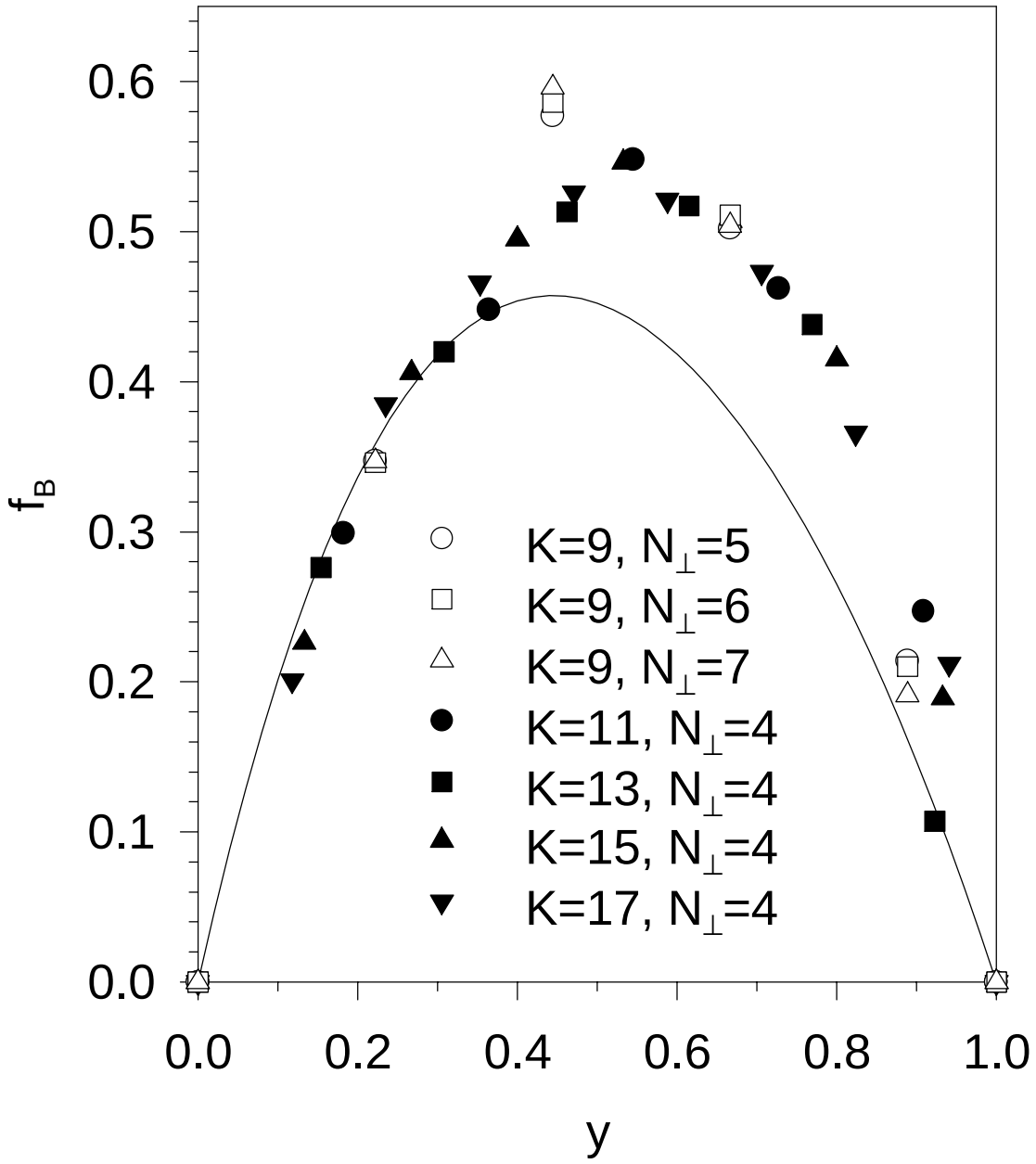

FIG. 5. Same as Fig. 3 but for $\langle :\phi^2(0):\rangle = 2$.

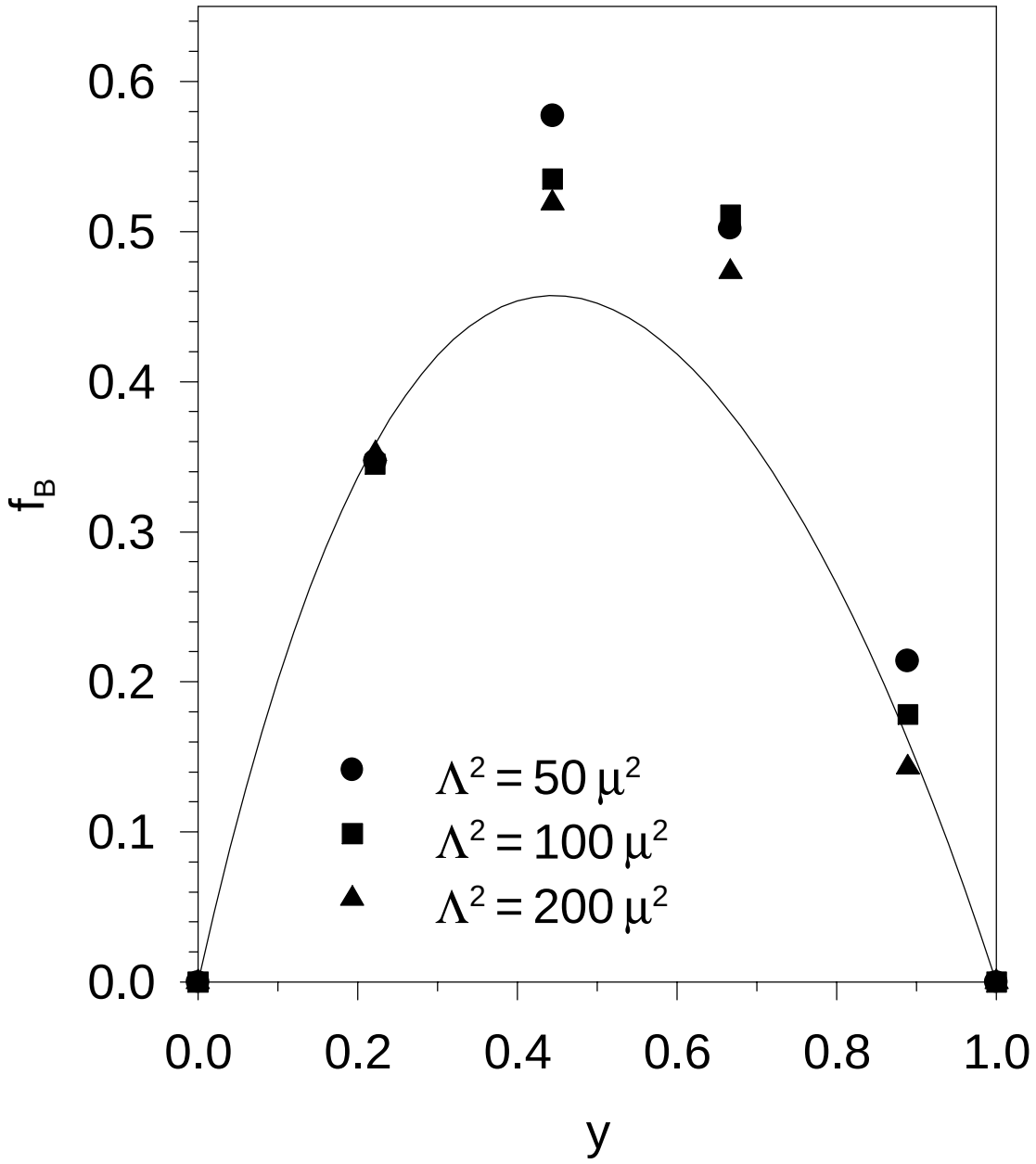

FIG. 6. Same as Fig. 4 but for $\langle :\phi^2(0): \rangle = 2$.

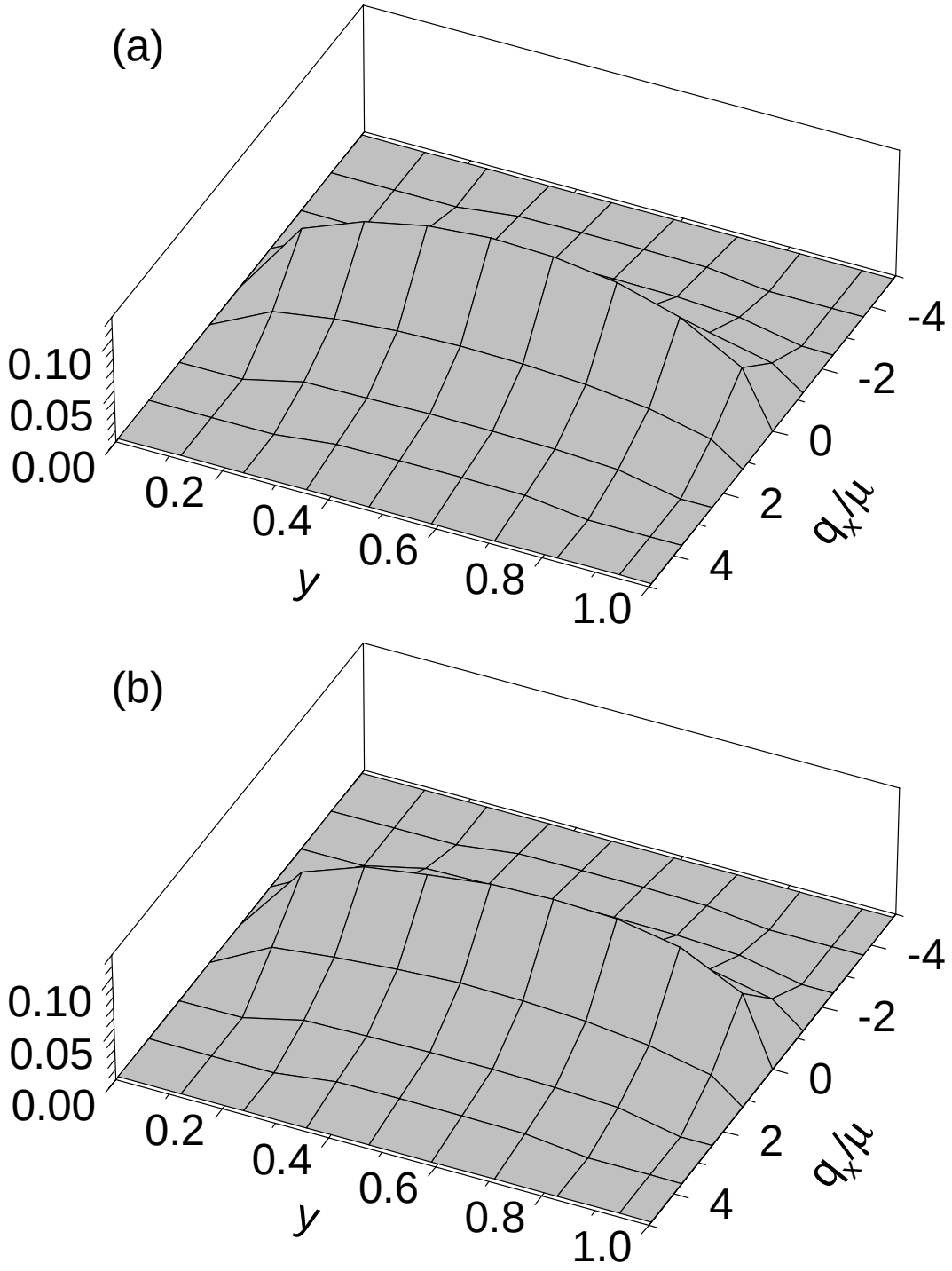

FIG. 7. The one-boson amplitude $\psi^{(1,0)}$ as a function of longitudinal momentum fraction y and one transverse momentum component q_x in the $q_y = 0$ plane. The analytic result is shown in (a) and the numerical result in (b) for $\Lambda^2 = 50\mu^2$, $K = 17$, and $N_\perp = 4$. Both correspond to $\langle{:}\phi^2(0){:}\rangle = 1$.

V. CONCLUSION

In this paper we present a new method for the renormalization of Hamiltonian light-cone-quantized field theories that maintains Lorentz invariance and other symmetries. The main difficulty which is confronted by such methods is the construction of the counterterms. We employ the traditional generalized Pauli–Villars method [6]. With a sufficient number of Pauli–Villars fields, perturbation theory is regulated while Lorentz symmetries and discrete symmetries are preserved with a minimal number of counterterms. These counterterms are generated automatically. We hypothesize that these counterterms are sufficient to regulate the nonperturbative problem.

In Yukawa theory, Pauli–Villars regularization preserves chiral symmetry [11,12], unlike the invariant-mass regulator. A similar outcome arises in QED where one needs Pauli–Villars regularization of the vacuum polarization loop to recover its vanishing at $q^2 \to 0$ [21]. These examples show that a covariant method is necessary in the nonperturbative context to find all counterterms.

Given that the theory is finite by suitable Pauli–Villars regularization, we can impose a regulator to limit the Fock space so as to produce a tractable numerical problem. A finite matrix approximation can then be obtained with use of the DLCQ procedure [1]. In the finite matrix problem we face the numerical difficulties of non-Hermitian matrices and large basis sizes. These difficulties are successfully addressed in a $3+1$-dimensional model [9] constructed to have an analytic solution. This model requires one Pauli–Villars boson as a regulator. We also study the DLCQ approximation to the one-loop fermion self energy in Yukawa theory, where three Pauli–Villars bosons are needed [11].

The non-Hermitian matrices are handled by the complex symmetric Lanczos diagonalization algorithm [18–20]. This technique is ideal for the extraction of extreme eigenvalues and their eigenvectors. It takes full advantage of the sparsity of the Hamiltonian matrix. For a given basis size, storage requirements are minimized.

The basis sizes required in the calculation are reasonable. The presence of Pauli–Villars particles, at the chosen mass and cutoff values, increased the model basis by only 100% and the loop-calculation basis by 150%. Given the sparsity of the matrix, increases of these magnitudes are quite acceptable. However, smooth convergence and extrapolation from bases of minimal size require the introduction of special integral weighting methods to DLCQ. The dramatic improvement which can occur is illustrated in Fig. 1.

With these methods we have obtained agreement between the numerical and analytic solutions of our model. The convergence of the numerical result in longitudinal and transverse resolution is remarkably rapid. The result is sensitive only to the cutoff used to limit the Fock space, but even there the convergence to the analytic result is clear. The methods seem well suited to situations where low-mass states have a small mean number of constituents. [22]

The natural next step is to extend the model toward a more realistic theory, namely Yukawa theory. The fermion can be given proper dynamics, and Yukawa-type interactions can be reintroduced. Once Yukawa theory itself can be studied with our nonperturbative method, there may be useful applications to the Higgs sector of the Standard Model. We are sufficiently encouraged by the success of the Pauli–Villars program for the examples discussed here to believe that it will have general applicability to QCD in $3+1$ dimensions.

ACKNOWLEDGMENTS

This work was supported in part by the Minnesota Supercomputer Institute through grants of computing time and by the Department of Energy. The hospitality of the Telluride Summer Research Center was also appreciated.

APPENDIX A: LIGHT-CONE COORDINATES

We define light-cone coordinates [23] by

$$x^{\pm} \equiv x^0 \pm x^3, \tag{A1}$$

with the transverse coordinates $\boldsymbol{x}_\perp \equiv (x^1, x^2)$ unchanged. Covariant four-vectors are written as *e.g.* $x^\mu = (x^+, x^-, \boldsymbol{x}_\perp)$, with the spacetime metric

$$g^{\mu\nu} = \begin{pmatrix} 0 & 2 & 0 & 0 \\ 2 & 0 & 0 & 0 \\ 0 & 0 & -1 & 0 \\ 0 & 0 & 0 & -1 \end{pmatrix}. \tag{A2}$$

Explicitly,

$$x \cdot y = g_{\mu\nu} x^\mu y^\nu = \frac{1}{2}(x^+ y^- + x^- y^+) - \boldsymbol{x}_\perp \cdot \boldsymbol{y}_\perp. \tag{A3}$$

We also make use of an underscore notation: for position-space variables we write

$$\underline{x} \equiv (x^-, \boldsymbol{x}_\perp), \tag{A4}$$

while for momentum-space variables

$$\underline{k} \equiv (k^+, \boldsymbol{k}_\perp). \tag{A5}$$

Then

$$\underline{k} \cdot \underline{x} \equiv \frac{1}{2} k^+ x^- - \boldsymbol{k}_\perp \cdot \boldsymbol{x}_\perp. \tag{A6}$$

Spatial derivatives are defined by

$$\partial_+ \equiv \frac{\partial}{\partial x^+}, \qquad \partial_- \equiv \frac{\partial}{\partial x^-}, \qquad \partial_i \equiv \frac{\partial}{\partial x^i}. \tag{A7}$$

The gamma matrices $\gamma^\pm \equiv \gamma^0 \pm \gamma^3 = (\gamma^\mp)^\dagger$ satisfy the familiar relation

$$\{\gamma^\mu, \gamma^\nu\} = 2g^{\mu\nu} \tag{A8}$$

with $g^{\mu\nu}$ the light-cone metric . It is simple to verify that the (Hermitian) matrices

$$\Lambda_\pm \equiv \frac{1}{2}\gamma^0\gamma^\pm \tag{A9}$$

satisfy

$$\Lambda_\pm^2 = \Lambda_\pm \ , \qquad \Lambda_\pm\Lambda_\mp = 0\,, \qquad \Lambda_+ + \Lambda_- = 1, \tag{A10}$$

so that they serve as projectors on spinor space. In the Dirac representation of the γ-matrices:

$$\Lambda_+ = \frac{1}{2}\begin{pmatrix} 1 & 0 & 1 & 0 \\ 0 & 1 & 0 & -1 \\ 1 & 0 & 1 & 0 \\ 0 & -1 & 0 & 1 \end{pmatrix}, \tag{A11}$$

which has two eigenvectors, both with eigenvalue $+1$:

$$\chi_{+\frac{1}{2}} = \frac{1}{\sqrt{2}}\begin{pmatrix} 1 \\ 0 \\ 1 \\ 0 \end{pmatrix} \qquad\qquad \chi_{-\frac{1}{2}} = \frac{1}{\sqrt{2}}\begin{pmatrix} 0 \\ 1 \\ 0 \\ -1 \end{pmatrix}. \tag{A12}$$

These serve as a convenient spinor basis for the expansion of the field $\psi_+ \equiv \Lambda_+\psi$ on the light cone.

APPENDIX B: WEIGHTING METHODS

New weighting schemes have now been developed for use with the DLCQ grid. They are based on extensions of the trapezoidal rule and Simpson's rule to the situation where the integration domain does not end on a grid point; they are also related to open Newton–Cotes formulas. The basic approach is to derive formulas for one-dimensional integrals and then iterate them for higher-dimensional integrals [15].

The extended trapezoidal rule is obtained from consideration of an integral from, say, x_0 to x_3. The relevant graph is shown in Fig. 8. The grid points are at x_1 and x_2, which are separated by a standard spacing h. The other points are at the integration domain boundaries at distances of h_L and h_R from the grid points. The integral of a function f is then approximated by

$$\int_{x_0}^{x_3} f dx \simeq a_1 f(x_1) + a_2 f(x_2)\,, \tag{B1}$$

with

$$\begin{aligned} a_1 &= (h + h_L + h_R)(h + h_L - h_R)/2h\,, \\ a_2 &= (h + h_L + h_R)(h + h_R - h_L)/2h\,. \end{aligned} \tag{B2}$$

The coefficients a_i are chosen to provide exact results for linear functions. The standard trapezoidal rule is recovered when $h_L = h_R = 0$. If $h_L = h_R = h$, a standard open

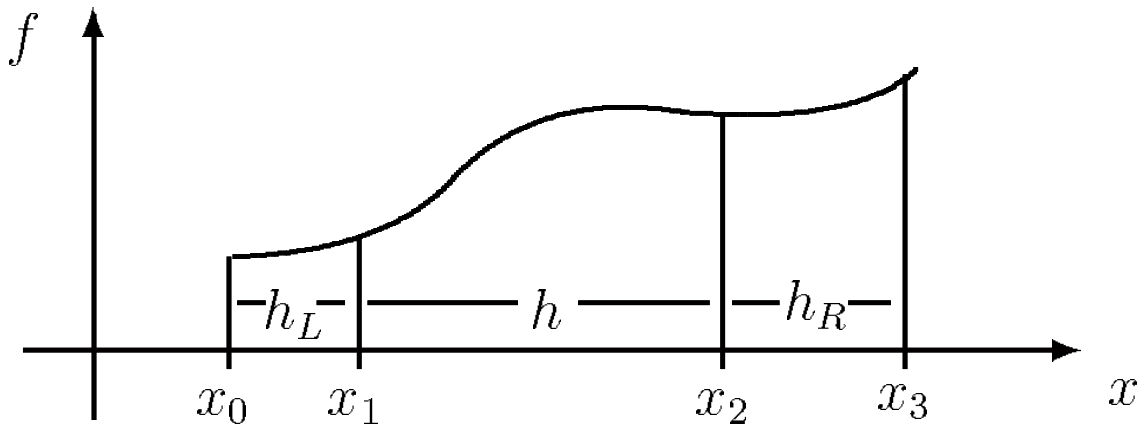

FIG. 8. Spacing of grid points for an arbitrary function.

Newton-Cotes formula results. When the extended rule is combined with the standard rule for interior intervals, a general composite rule is obtained. The extended rule is then used twice, once at each end, with h_R or h_L set to zero.

The extended Simpson's rule follows from similar steps. Two forms are needed, one for three grid points and another for four. Any situation with more grid points can be handled with a composite rule obtained by combining these rules with the standard Simpson's rule. For the three-point case, consider an integral from x_0 to x_4, with grid points at x_1, x_2, and x_3. The regular grid spacing is h; the extra points at the beginning and end are separated by h_L and h_R, respectively. The approximation to the integral is then

$$\int_{x_0}^{x_4} f dx \simeq a_1 f(x_1) + a_2 f(x_2) + a_3 f(x_3)\,, \tag{B3}$$

where

$$\begin{aligned} a_1 &= (4h^3 + 12h^2 h_L + 9hh_L^2 + 2h_L^3 + 3hh_R^2 + 2h_R^3)/12h^2\,, \\ a_2 &= (4h^3 - 3hh_L^2 - h_L^3 - 3hh_R^2 - h_R^3)/3h^2\,, \\ a_3 &= (4h^3 + 12h^2 h_R + 9hh_R^2 + 2h_R^3 + 3hh_L^2 + 2h_L^3)/12h^2\,. \end{aligned} \tag{B4}$$

These coefficients are constructed to provide exact results for quadratic functions. When $h_L = h_R = 0$ they reduce to the coefficients found in Simpson's rule, and, because of the greater symmetry, the rule becomes exact for cubic functions as well.

The four-point rule is also exact for cubic functions. It is

$$\int_{x_0}^{x_5} f dx \simeq a_1 f(x_1) + a_2 f(x_2) + a_3 f(x_3) + a_4 f(x_4)\,, \tag{B5}$$

where

$$
\begin{aligned}
a_1 &= (9h^4 + 24h^3 h_L + 22h^2 h_L^2 + 8h h_L^3 + h_L^4 - 4h^2 h_R^2 - 4h h_R^3 - h_R^4)/24h^3 \,, \\
a_2 &= (27h^4 - 36h^2 h_L^2 - 20h h_L^3 - 3h_L^4 + 18h^2 h_R^2 + 16h h_R^3 + 3h_R^4)/24h^3 \,, \\
a_3 &= (27h^4 - 36h^2 h_R^2 - 20h h_R^3 - 3h_R^4 + 18h^2 h_L^2 + 16h h_L^3 + 3h_L^4)/24h^3 \,, \\
a_4 &= (9h^4 + 24h^3 h_R + 22h^2 h_R^2 + 8h h_R^3 + h_R^4 - 4h^2 h_L^2 - 4h h_L^3 - h_L^4)/24h^3 \,.
\end{aligned}
\tag{B6}
$$

These integration formulas greatly reduce the size of the errors, as shown for the extended trapezoidal rule (B1) in Fig. 9, but they do not result in systematic behavior. The lack of systematic dependence is primarily due to the use of a square grid to approximate a circular domain in the transverse direction. One way of putting this is that the iterated Cartesian integrals try to approximate π (a key factor in the area of the circle) as well as approximate the integral itself.

To overcome this square/circle problem, the integral is written in polar coordinates

$$
\int dxdy f(x,y) = \frac{1}{2}\int_0^{2\pi} d\phi \int_0^{R^2} d(r^2)\tilde{f}(r^2,\phi)\,. \tag{B7}
$$

The points of the square grid lie on circles of varying radii r_i shown in Fig. 10. The r_i are easily computed from the coordinates of the square grid. The squares of these radii are used as the grid points for a trapezoidal approximation to the radial (r^2) integral. Because the limit R^2 does not fall on one of these points, the extended trapezoidal rule (B1) must be used for the last interval. Clearly, the intervals are not of equal length; however, they are on average of order $3h^2$, where h is the spacing in the square grid. For the first 10 circles, the average spacing in r^2 is actually closer to $2h^2$.

The number of points on the square grid that fall on any one circle come in multiples of 4, because of reflection symmetries. These points can be used to approximate the angular integral on each circle via another application of the trapezoidal rule. For the self-energy integral I, however, the integrand is independent of angle and one can simply use one point or average the values at all points. The contribution to the weighting of a grid point is then the same for all transverse points on the same circle.

The circular weighting in the transverse direction can be combined with either the extended trapezoidal rule or the extended Simpson's rule in the longitudinal direction. A comparison of the two is shown in Fig. 11. The relatively large excursions for small $N_\perp$ are due to the small number of grid points involved for this case of a large boson mass. For larger $N_\perp$ the extended Simpson's rule is seen to result in less excursion between different values of K, and is preferred for the self-energy integral. Results for the extended Simpson's rule are compared with those of the ordinary DLCQ sum in Fig. 1; in this case the results for the extended trapezoidal rule would not be visibly worse.

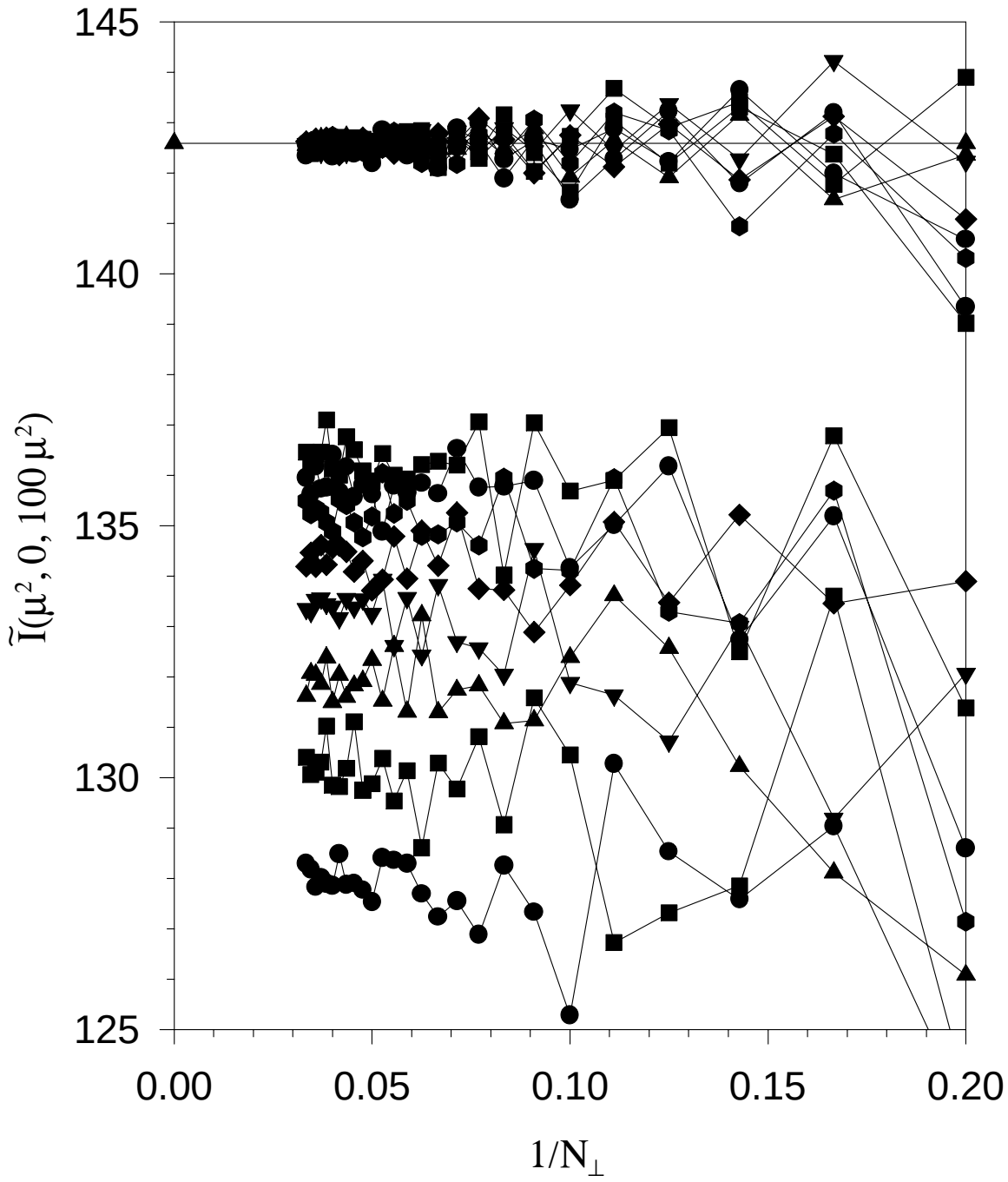

FIG. 9. Same as Fig. 1 except that the numerical values oscillating about the analytic answer are computed without transverse circular weighting and with only trapezoidal weighting in the longitudinal and transverse directions. The lack of circular weighting destroys the smoothness of the results shown in Fig. 1.

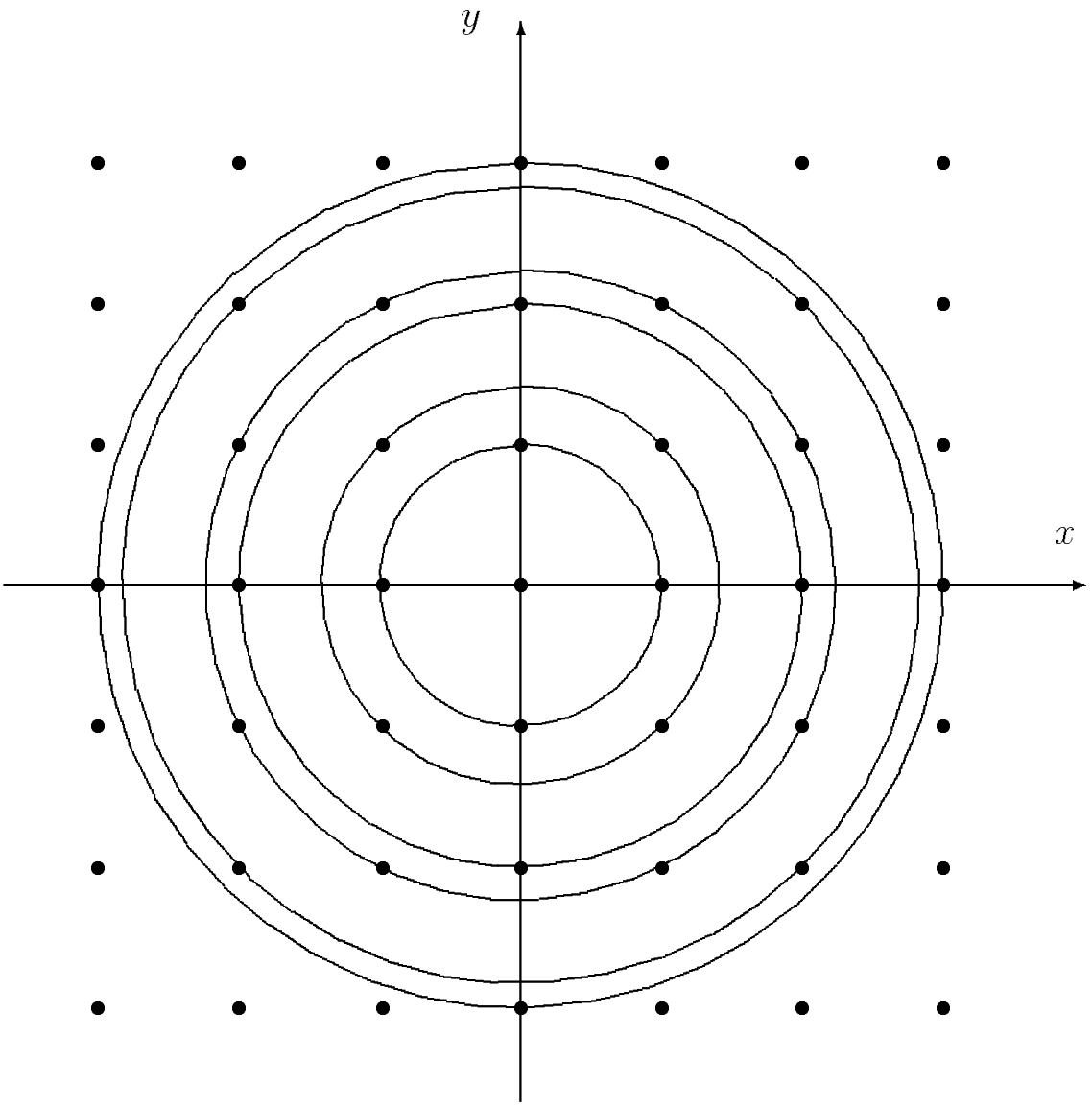

FIG. 10. Square transverse grid with points on circles of varying radii.

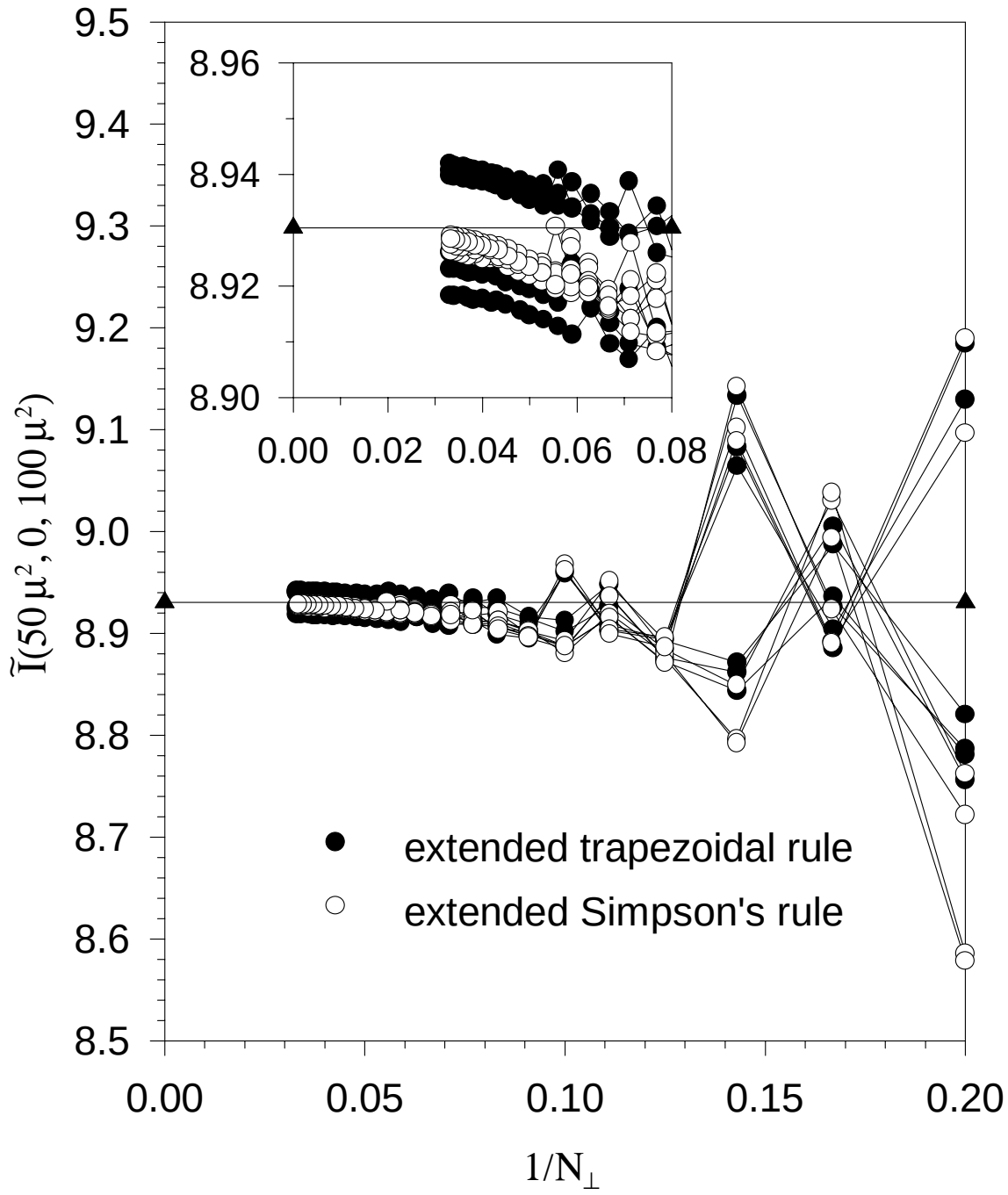

FIG. 11. One-loop fermion self energy. Results for the extended trapezoidal and Simpson rules are compared. The horizontal line is the exact result. The DLCQ grid parameters take the ranges $K = 20, 21, \ldots, 25$ and $N_\perp = 5, 6, \ldots, 30$. Points calculated with the same value of K are connected by lines.

REFERENCES

[1] H.-C. Pauli and S.J. Brodsky, Phys. Rev. D **32**, 1993 (1985); **32**, 2001 (1985).

[2] For reviews, see S.J. Brodsky and H.-C. Pauli, in *Recent Aspects of Quantum Fields*, edited by H. Mitter and H. Gausterer, Lecture Notes in Physics Vol. 396 (Springer-Verlag, Berlin, 1991); S.J. Brodsky, G. McCartor, H.-C. Pauli, and S.S. Pinsky, Part. World **3**, 109 (1993); M. Burkardt, Adv. Nucl. Phys. **23**, 1 (1996).

[3] For a recent DLCQ calculation, see D.J. Gross, A. Hashimoto, and I.R. Klebanov, NSF-ITP-97-133, hep-th/9710240, 1997, unpublished.

[4] See, for example, M. Krautgartner, H.-C. Pauli, and F. Wölz, Phys. Rev. D **45**, 3755 (1991).

[5] K.G. Wilson, T.S. Walhout, A. Harindranath, W.-M. Zhang, R.J. Perry, and St.D. Głazek, Phys. Rev. D **49**, 6720 (1994); St.D. Głazek and K.G. Wilson, Phys. Rev. D **48**, 5863 (1993); **49**, 4214 (1994); M. Brisudová and R.J. Perry, Phys. Rev. D **54**, 1831 (1996); M. Brisudová and R.J. Perry, *ibid.* **54**, 6453 (1996); M. Brisudová, R.J. Perry, and K.G. Wilson, Phys. Rev. Lett. **78**, 1227 (1997); B.D. Jones, R.J. Perry, and St.D. Głazek, Phys. Rev. D **55**, 6561 (1997); B.D. Jones and R.J. Perry, *ibid.*, 7715 (1997). See also K. Harada and A. Okazaki, *ibid.*, 6198 (1997); E.L. Gubankova and F. Wegner, hep-th/9702162, 1997, unpublished.

[6] W. Pauli and F. Villars, Rev. Mod. Phys. **21**, 4334 (1949).

[7] For a light-cone bound-state calculation in Yukawa theory, see St. Głazek, A. Harindranath, S. Pinsky, J. Shigemitsu, and K. Wilson, Phys. Rev. D **47**, 1599 (1993); P.M. Wort, *ibid.* **47**, 608 (1993).

[8] S.-J. Chang and T.-M. Yan, Phys. Rev. D **7**, 1133 (1973); M. Burkardt and A. Langnau, Phys. Rev. D **44**, 3857 (1991).

[9] O.W. Greenberg and S.S. Schweber, Nuovo Cim. **8**, 378 (1958); S.S. Schweber, *An introduction to relativistic quantum field theory*, (Row, Peterson, Evanston, IL, 1961), p. 339.

[10] G.P. Lepage and S.J. Brodsky, Phys. Rev. D **22**, 2157 (1980).

[11] C. Bouchiat, P. Fayet, and N. Sourlas, Lett. Nuovo Cim. **4**, 9 (1972); S.-J. Chang and T.-M. Yan, Phys. Rev. D **7**, 1147 (1973).

[12] M. Burkardt and A. Langnau, Phys. Rev. D **44**, 1187 (1991).

[13] D.G. Robertson and G. McCartor, Z. Phys. C **53**, 661 (1992).

[14] G. McCartor and D.G. Robertson, Z. Phys. C **53** 679 (1992).

[15] For a similar approach to iterated integrals in the context of fast fourier transforms, see P. Luchini, Comput. Phys. Commun. **31**, 303 (1984).

[16] St.D. Głazek and R.J. Perry, Phys. Rev. D **45**, 3734 (1992).

[17] S.D. Drell and T.-M. Yan, Phys. Rev. Lett. **24**, 181 (1970); S.J. Brodsky and S.D. Drell, Phys. Rev. D **22**, 2236 (1980).

[18] C. Lanczos, J. Res. Nat. Bur. Stand. **45**, 255 (1950); J.H. Wilkinson, *The Algebraic Eigenvalue Problem* (Clarendon, Oxford, 1965); B.N. Parlett, *The Symmetric Eigenvalue Problem* (Prentice–Hall, Englewood Cliffs, NJ, 1980); J. Cullum and R.A. Willoughby, J. Comput. Phys. **44**, 329 (1981); *Lanczos Algorithms for Large Symmetric Eigenvalue Computations* (Birkhauser, Boston, 1985), Vol. I and II; D.S. Scott, in *Sparse Matrices and their Uses*, edited by I.S. Duff (Academic Press, London, 1981),

p. 139; G.H. Golub and C.F. van Loan, *Matrix Computations* (Johns Hopkins University Press, Baltimore, 1983); R.G. Grimes et al., J. Comput. Phys. **69**, 471 (1987); R.G. Grimes and H.D. Simon, J. Comput. Phys. **77**, 270 (1988); D.S. Scott, Comput. Phys. Commun. **53**, 271 (1989).

[19] J.H. Wilkinson, Ref. 18; Y. Saad, Comput. Phys. Commun. **53**, 71 (1989); S.K. Kin and A.T. Chronopoulos, J. Comp. and Appl. Math **42**, 357 (1992).

[20] J. Cullum and R.A. Willoughby, in *Large-Scale Eigenvalue Problems*, eds. J. Cullum and R.A. Willoughby, Math. Stud. **127** (Elsevier, Amsterdam, 1986), p. 193.

[21] S.J. Brodsky, R. Roskies, and R. Suaya, Phys. Rev. D **8**, 4574 (1973).

[22] K. Hornbostel, S.J. Brodsky, and H.-C. Pauli, Phys. Rev. D **41**, 3814 (1990); Ref. 3.

[23] P.A.M. Dirac, Rev. Mod. Phys. **21**, 392 (1949).